Techno-economic Comparison of Combined Cycle Gas Turbines with Advanced Membrane Configuration and Monoethanolamine Solvent at Part Load Conditions

Mijndert van der Spek,*[,†] Davide Bonalumi,[‡] Giampaolo Manzolini,[‡] Andrea Ramirez,[§] and André Faaij[∥]

[†]Copernicus Institute of Sustainable Development, Section Energy & Resources, Utrecht University, Heidelberglaan 2, 3584 CS Utrecht, The Netherlands

[‡]Dipartimento di Energia, Politecnico di Milano, Via Lambruschini 4, 20156 Milano, Italy

[§]Department of Energy Systems and Services, Section Energy & Industry, Delft University of Technology, Jaffalaan 5, 2628 BX Delft, The Netherlands

[∥]Center for Energy and Environmental Sciences, IVEM, University of Groningen, Nijenborgh 6, 9747 AG Groningen, The Netherlands

ABSTRACT: This work compares the part load techno-economic performance of CO_2 capture from a combined cycle gas turbine (CCGT) using a membrane configuration with selective CO_2 recycle and using monoethanolamine (MEA) solvent, under the assumption of flexible power plant dispatch. This is the first time that the techno-economic performance of CO_2 capture technologies is compared assuming a flexible dispatch profile, and the assessment was done using a comprehensive, new, part load assessment approach. Analyzing the part load performance of CO_2 capture and storage (CCS) technologies is relevant because of significant changes in our power systems, dramatically reducing the utilization of thermal power plants. The technical performance of the configurations with and without CCS was simulated at steady state, at operating points between maximum continuous rating (100% gas turbine loading) and minimum stable load (35% gas turbine loading). The performance at these operating points was then aggregated into weighted averages to produce single performance indicators (specific CO_2 intensity, specific primary energy per tonne of CO_2 avoided (SPECCA), and levelized cost of electricity (LCOE)) over the dispatch profile of the power plant. The technical performance of the MEA configuration was favorable over the membrane configuration over the whole CCGT loading range. The MEA SPECCA increased from 3.02 GJ/(t of CO_2) at 100% GT loading to 3.65 GJ/(t of CO_2) at 35% GT loading; the membrane SPECCA increased from 3.35 to 4.20 GJ/(t of CO_2). The higher SPECCA of the membrane configuration is caused by the reduced gas turbine efficiency, due to the selective recycling of CO_2 to the GT. When equal GT efficiency was assumed for combustion with normal air and with CO_2 enriched air, the membranes' technical performance was comparable with that of MEA. The capital costs of the CCGT with membrane configuration were 35% higher than the CCGT with MEA configuration. That, and the 6 year replacement frequency of the membranes, led the membrane LCOE to be 10 €/(MW h) higher than the MEA LCOE, when calculated with the part load approach. The membrane LCOE was 8 €/(MW h) higher when a full load was assumed. The new part load approach proved instrumental in highlighting performance (differences) at flexible dispatch conditions and aggregating those into easy to understand performance indicators.

INTRODUCTION

Techno-economic assessments of CO_2 capture technologies for the power sector are typically carried out assuming full load operation of the power and capture plants.[1−3] In reality, however, power plants are rarely fully dispatched and, rather, cycle up and down to match electricity supply and demand.[4−10] Among others due to overcapacity, European fossil-fueled power plants had an average capacity factor of just 34% in 2014.[11] In the U.S., coal-fired power plants reported 2011 capacity factors between 38 and 71%.[1] In the coming decades, this situation is expected to remain: although some redundant thermal generating capacity is expected to be taken offline, increasing grid penetration of intermittent renewables—among others—will require fossil power plants to continue to operate flexibly.[6−8,12]

This discrepancy between the technology assessment practice (full load) and real operation (part load) may pose a risk when comparing the feasibility of different CO_2 capture technologies and also when trying to optimize the initial design of a single CO_2 capture technology; it may be that the technology that seems most feasible under the assumption of full load is a lesser option when analyzed under realistic conditions.

In a previous communication, we proposed to assess and compare the techno-economic performance of CO_2 capture plants while explicitly including part load operation and using realistic dispatch assumptions.[5] In this work we follow up on that recommendation. One technology that may show favorable performance when operated at part load is the use of membranes for postcombustion CO_2 capture. Previous studies have already suggested that membranes may be competitive for CO_2

Received: July 17, 2017
Revised: November 27, 2017
Published: November 27, 2017

Table 1. Mathematical Representation of Techno-economic Calculations for the Part Load Approach and Comparison with the Conventional (Full Load) Approach[5]

	full load approach	part load techno-economic approach
E_{el} (MW h)[a]	$P_{des}\mathrm{HPY}_{tot}$	$\sum_{op=1}^{n} P_{op}\mathrm{HPY}_{op}$
CEI_{av} [kg/(MW h)][b]	$3600\frac{F_{CO_2,des}}{P_{des}}$	$\frac{3600(1+\alpha)}{\mathrm{HPY}_{tot}}\sum_{op=1}^{n}\left[\frac{F_{CO_2,op}\mathrm{HPY}_{op}}{P_{op}}\right]$
SPECCA_{av} [GJ/(t of CO_2)][c]	$3600\frac{\left(\frac{1}{\eta_{cc,des}}-\frac{1}{\eta_{ref,des}}\right)}{\mathrm{CEI}_{ref,des}-\mathrm{CEI}_{cc,des}}$	$\frac{3600}{\mathrm{HPY}_{tot}}\frac{\sum_{op=0}^{n}\left[\mathrm{HPY}_{op}\left(\frac{1}{\eta_{cc,op}}-\frac{1}{\eta_{ref,op}}\right)\right]}{\mathrm{CEI}_{ref,av}-\mathrm{CEI}_{cc,av}}$
levelized cost of electricity [€/(MW h)][d]	$\frac{\sum_t\left[\frac{\text{cash flow}_t}{(1+r)^t}\right]}{\sum_t\left[\frac{P_{des}\mathrm{HPY}_{tot}}{(1+r)^t}\right]}$	$\frac{\sum_t\left[\frac{\text{cash flow}_t}{(1+r)^t}\right]}{\sum_t\left[\frac{\sum_{op=1}^{n}P_{op}\mathrm{HPY}_{op}}{(1+r)^t}\right]}$

[a] E = electricity produced: where P_{des} and P_{op} are the power output at the design or the operating point in MW, HPY_{op} are the hours per year that the plant runs at the respective operating point, and HPY_{tot} is the total hours per year that the plant is in operation. [b] CEI_{av} = average CO_2 emission intensity: where F_{CO_2} are the CO_2 emissions (kg/s) at design or operating point; P_{des} and P_{op} are the power output at the design or the operating point (MW); HPY_{op} are the hours per year that the plant runs at the respective operating point; HPY_{tot} is the total hours per year that the plant is in operation, excluding the hours that the plant stands idle. It is optional to include a value for the coefficient α representing any additional CO_2 emissions as a result of plant cycling that are not included in the steady state performance evaluations. This could be retrieved from actual plant emissions data. [c] SPECCA_{av}: where η is the net plant efficiency both with (cc) and without CCS (ref) and subscripts des and op refer to conditions at design and operating points. [d] Levelized cost of electricity: where r is the discount rate used to calculate the value of cash flows in year t. Cash flows include investment costs (IC), fixed and variable operation and maintenance costs (FOM, VOM), fuel costs (FC), and restart costs (RC) as follows:

$$\text{cash flow}_t = \left[\mathrm{IC} + \mathrm{FOM} + \sum_{op=1}^{n}(\mathrm{VOM}+\mathrm{FC})_{op} + \mathrm{RC}\right]_t$$

separation from power plant flue gases at full load.[13−16] Due to the characteristics of membranes, it is expected that their competitiveness further improves if power plants are operated at part load: at part load the flue gas flow of a power plant is reduced, but since the same absolute membrane surface area is available, this leads to a higher specific surface area per cubic meter of flue gas. Flue gas velocities over the membrane will thus be lower, resulting in increased species flux. This may allow lower pressure ratios over the membrane, reducing the specific compression energy required to capture a unit of CO_2. Conversely, the specific energy consumption of postcombustion solvents is expected to remain the same or increase at part load, because of being limited by chemical equilibrium and regeneration constraints; e.g., see ref 14.

In this context, this work starts from the hypothesis that the relative energy performance of postcombustion membranes versus postcombustion solvents improves at part load due to increased species flux through the membrane, resulting in lower compression requirements. This should also lead to improved economic performance at part load, because of reduced specific energy costs of capture. We set out to test this hypothesis using a framework for techno-economic analysis of CO_2 capture technologies that explicitly considers real(istic) dispatch profiles of CCS power plants, including part load operation (earlier presented in ref 5). CO_2 capture from a natural gas fired combined cycle was assumed, because these plants are expected to cycle more than coal power plants (although coal is also expected to cycle somewhat[7]). The analysis includes a detailed description of operating strategies, technical performance, and technical (im)possibilities when operating membranes and MEA plants at part load, fostering enhanced understanding of part load operation of power plants with CCS.

METHODOLOGICAL FRAMEWORK

We applied the methodological framework we presented in ref 5, which aims to facilitate power and CO_2 capture plant techno-economic analysis while explicitly considering realistic plant dispatch and part load performance. Using the framework, we analyzed the CCS power plant performance based on discretized operating profiles (plant operating point or loading versus hours that it operates at this operating point) that are representative of commercial power plant operations. The CCS power plant was analyzed using steady state simulations (see CCGT Modeling) of its performance at five operating points, analogous to those from ref 17 and as suggested in ref 5. These operating points were selected based on the gas turbine design output, and its minimum turndown: 35%, 40%, 60%, 80%, and 100% of GT design output.

The novelty of this method is that it combines the performance of the five operating points into single weighted average performance indicators and that it also includes the economic performance of the flexible CCS power plant, thereby allowing techno-economic comparison of different carbon capture technologies. The selected performance indicators included annual produced electricity, average CO_2 emission intensity, average SPECCA (specific primary energy consumption per tonne of CO_2 avoided), and levelized cost of electricity. These indicators were selected because they are widely applied in techno-economic assessment of CCS power[1,2,18,19] and are therefore well understood by researchers, industry, and policy makers. The equations for calculation of the performance indicators using the part load techno-economic approach are presented in Table 1.

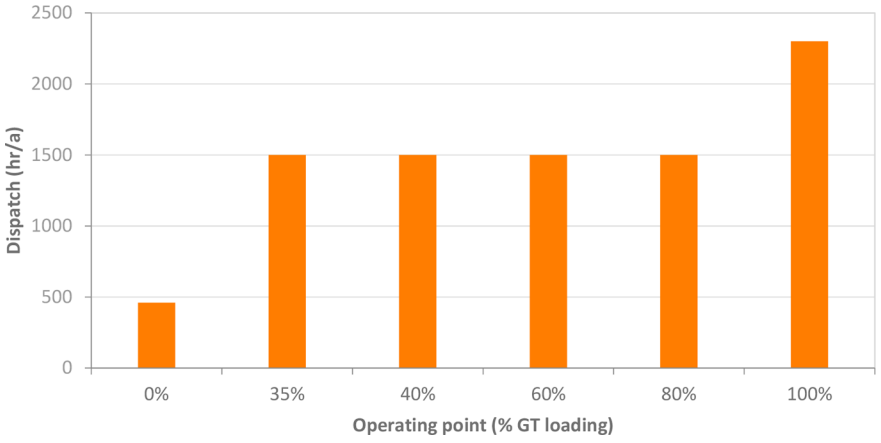

Figure 1. Hypothetical dispatch profile that was used to calculate the part load techno-economics. It was based on a modeled 2050 scenario with 60% renewable electricity sources,[20] including 41% intermittent renewables, leading to an average CCGT with CCS capacity factor of 63% for West-European countries.

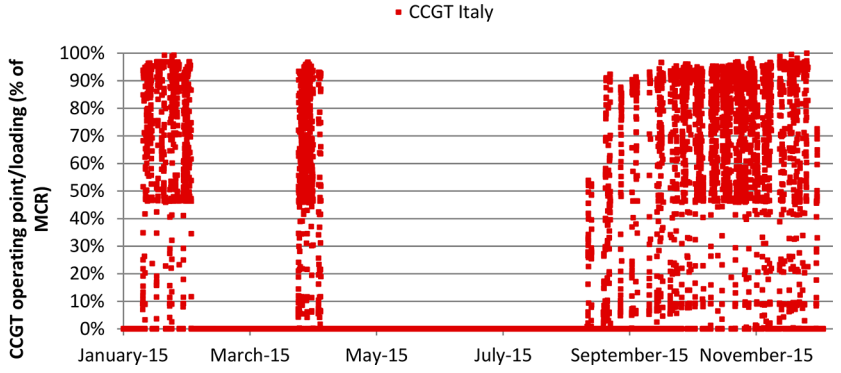

Figure 2. Dispatch profile of an Italian CCGT over the year 2015, (percent output of MCR, 15 min time interval). Note that the plant had a very low utilization, leading to a capacity factor of 16%. This was representative of the European situation in 2015 with large overcapacity, low coal prices, and high natural gas prices. Also note that the plant cycles up and down considerably, which stresses the relevance of assessing CCS plant performance including part load operation (data source, the plant owner; similar data retrievable from the ENTSO-E transparency platform).

DISPATCH PROFILES

The equations in Table 1 require weighing of performance, based on the hours that the plant is dispatched at a specific operating point. The part load method thus requires the definition of a dispatch profile, which can be defined in three ways: the first option involves the modeling of future dispatch profiles using power plant scheduling models such as the unit commitment capacity optimization (UCCO) model[8] or the REPOWERS model.[12] A second option is to acquire a recent dispatch profile, or set of dispatch profiles, of an existing power plant, e.g., from operating companies or via electricity system performance databases such as the European ENTSO-E transparency platform.[11] A third option is to assume a hypothetical profile, for instance based on either of the two options above.

In this work, we used a hypothetical profile (Figure 1) that was based on electricity system modeling by Brouwer et al.[20] The profile is representative of a 2050 scenario with 60% renewable electricity production, including 41% intermittent renewables. The scenario includes the countries of Western Europe—Scandinavia, the British Isles, Germany and the Benelux, France, the Iberian Peninsula, and Italy and the alpine states—and predicts an average capacity factor of 63% for CCGTs with CCS. Note that this capacity factor is still fairly high because the model converges to economically optimal construction and dispatch of power generators and it minimizes idle time of assets, while maximizing the economically optimal use of (intermittent) renewables. The model predicts dispatch of generators as a group, and not per individual unit, which may also lead to higher average capacity factors. As a sensitivity, we applied a dispatch profile based on a 2050 scenario for the U.K. by Mac Dowell and Staffell,[8] which does include the dispatch of individual generators and predicts an average CCGT with CCS capacity factor of 42%. We also included a full load scenario (85% CF) and a real Italian 2015 dispatch profile as sensitivities. The latter has a very low capacity factor of 16%, and is representative of an electricity system with large overcapacity and high natural gas prices (Figure 2).

TECHNOLOGY DESCRIPTION

The technologies that were compared in this work included postcombustion CO_2 capture with polymeric membranes and postcombustion capture with MEA solvent. Both capture technologies were integrated with a combined cycle gas turbine power plant, which follows the design specifications and boundary conditions of the European Benchmarking Task Force (EBTF; see refs 18, 21, and 22 and Table 2).

CCGT WITH MEMBRANE CONFIGURATION

The membrane configuration analyzed in this work is an advanced cycle, including selective recycling of CO_2 to the gas turbine to increase the CO_2 concentration in the flue gas to about 25% on a volume basis, thus allowing easier separation by

Table 2. Modeling Specifications and Assumptions Based on the EBTF[18]

parameter	value
natural gas	
molar composition (%)	
CH_4, C_2H_6, C_3H_8, C_4H_{10}, CO_2, N_2	89, 7, 1, 0.1, 2, 0.9
lower heating value (MJ/kg)	46.50
higher heating value (MJ/kg)	51.47
CO_2 emission factor (g_{CO_2}/MJ_{LHV})	56.99
gas turbine	
type	GE9371FB
compressor pressure ratio	18.2
TIT (turbine inlet temperature, °C)	1427
TOT (turbine outlet temperature, °C)	646
GT gross LHV efficiency (%)	37.9
air inlet filter pressure drop (mbar)	10
temperature of fuel to combustor (°C)	160
shaft mechanical efficiency (%)	modeled
generator electrical efficiency (%)	modeled
steam cycle	
evaporation pressure levels (bar)	130/28/4
maximum SH/RH steam temperature (°C)	565
minimum approach point ΔT in SH/RH (°C)	25
pinch point ΔT in HRSG (°C)	10
liquid subcooling ΔT at drum inlet (°C)	5
heat losses, % of heat transferred	modeled
gas side pressure loss in HRSG (kPa)	modeled
HP SH pressure loss (%)	modeled
HP/IP pumps hydraulic efficiency (%)	85/75
HP/IP/LP turbine isentropic efficiency (%)	modeled
turbine shaft mechanical efficiency (%)	modeled
generator electrical efficiency (%)	98.94
condensing pressure (bar)	0.048
flue gas compressor and expander	
pressure ratio	2
compressor polytropic efficiency (%)	80
expander polytropic efficiency (%)	94
mechanical efficiency (%)	99.6
CO_2 purification and compression	
low temperature flash temperature (°C)	<−55
high temperature flash temperature (°C)	−33
pressure at LT flash inlet (bar)	30.0
minimum ΔT in low temperature heat exchangers (°C)	3
no. of intercooled compression stages	4
isentropic efficiency (%)	80
mechanical efficiency (%)	99.6
intercoolers outlet temperature (°C)	30
intercoolers pressure losses (%)	2
liquid CO_2 temperature (°C)	30
CO_2 vacuum pump	
gas pressure at vacuum pump inlet (bar)	0.2
no. of intercooled stages	2
isentropic efficiency (%)	80
mechanical/electrical efficiency (%)	99.6
intercoolers outlet temperature (°C)	30

the CO_2 capture membrane (Figure 3). This is called selective exhaust gas recycling (SEGR). SEGR in combination with post-combustion membranes was earlier analyzed at full load by Merkel et al.[13] and Turi et al.[15] and was found to be competitive with MEA at full load. In the cycle, CO_2 enriched air (15−20%$_{vol}$ CO_2; streams 3 and 4) is sent to the gas turbine where preheated natural gas (stream 17) is burnt. The gas turbine exhaust gas is used to provide heat to the steam cycle in the heat recovery steam generator (HRSG; stream 7), after which it is further cooled in a direct contact cooler (DCC; stream 8). The CO_2 rich flue gas (20−25%$_{vol}$ CO_2) is then compressed to 2 bar (stream 10), and part of the CO_2 (∼17%) is separated in the CO_2 capture membrane (CCM; stream 14). The permeate side of the CCM is operated at vacuum conditions to create a driving force for CO_2 separation. The permeate is subsequently sent to the compression and purification unit (CPU; stream 15),

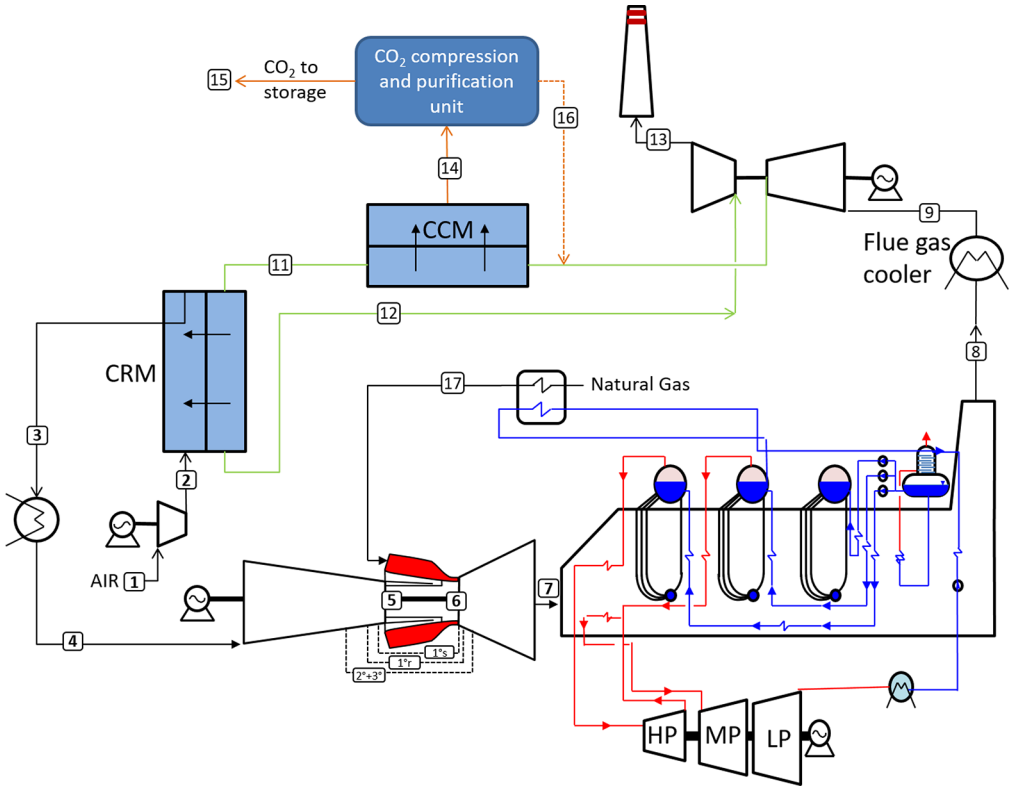

Figure 3. PFD of the advanced CCGT membrane configuration, including selective exhaust gas recycle. The figure shows the gas turbine, HRSG, steam turbines, and the recycle with compressors/expander, membranes, and CO_2 compression and purification unit. The membranes include the CCM (CO_2 capture membrane) and the CRM (CO_2 recycle membrane). Based on information from ref 15.

where the inerts (AR, N_2, and O_2) are removed and the CO_2 is compressed to pipeline specifications of 110 bar. The flue gas (retentate, still containing 15–20% CO_2) is further treated in the CO_2 recycle membrane (CRM), where the remainder of the CO_2 is removed to render a CO_2 lean flue gas (stream 12).

The flue gas is still at elevated pressure, and part of its mechanical energy is recovered in an expander, after which the gas is vented (stream 13). The CRM operates with the combustion air as sweep gas (streams 1 and 2), rather than with a vacuum at the permeate side. In this way, the combustion air only needs slight pressurization to overcome the pressure drop over the membrane, which is energetically favorable over creating a vacuum. After the CRM, the CO_2 enriched combustion air is cooled and water vapor is knocked out, before it is fed to the gas turbine.

For postcombustion CO_2 capture with membranes, polymer membranes represent the state of the art.[23] The type closest to commercialization (TRL 7) is the Polaris membrane developed by membrane technology research (MTR), which has been tested in large pilot plants fed by coal flue gas equivalent to 1 MW electricity output.[13] Other emerging postcombustion membrane types exist,[23] such as facilitated transport membranes,[24−26] which have the advantage of a higher selectivity of CO_2 versus nitrogen but are far less developed (TRL 3–6). For the purpose of comparing part load operation of membranes and solvents, we chose to use the current state of the art and, thus, the Polaris membranes.

CCGT WITH MEA CONFIGURATION

The CCGT with MEA configuration also considers exhaust gas recycling (EGR), contrary to the reference cases in the previous studies. This allows comparison with the membrane configuration to be on a more like-for-like basis. Exhaust gas recycling decreases the flue gas flow to the CO_2 capture unit with values of about 40%, while increasing its CO_2 content to 6–7%$_{vol}$.[27−30] The benefits are therefore 2-fold: lower flue gas flows allow for smaller absorbers (approximately half the volume compared to a situation without EGR), and the equilibrium specific CO_2 separation energy approaches that of coal flue gas, thereby increasing the net efficiency of a CCGT with MEA configuration by around 1% point.[27,31]

Figure 4 shows the process flow diagram of the CCGT with EGR and MEA postcombustion capture. Just like in the membrane configuration, natural gas is combusted in the gas turbine using CO_2 enriched air (~3% CO_2, stream 2). After passing through the HRSG (stream 5), the flue gas is cooled to 40 °C in a DCC (stream 6). A 35% amount of the flue gas is recycled back to the gas turbine (stream 10), while the remainder continues to the MEA plant (stream 7). Higher recycle ratios are possible, but they only marginally increase energetic efficiency, while increasing the risk of CO and NO_x formation in the gas turbine combustion chamber.[30] The pressure drop in the DCC and absorber column are balanced by a recycle blower and a flue gas blower. The flue gas flows through the absorption column, where it is chemically bound to the MEA solvent, after which the CO_2 lean flue gas is vented (stream 8). The rich solvent is regenerated in a stripper, using steam from the HRSG IP/LP crossover. Both absorber and stripper contain water washes to reduce amine loss. The resulting CO_2 stream is dried and pressurized to 110 bar (stream 9).

PROCESS MODELING

The different parts of the CCGT-SEGR-membrane and the CCGT-EGR-MEA configurations were simulated using different

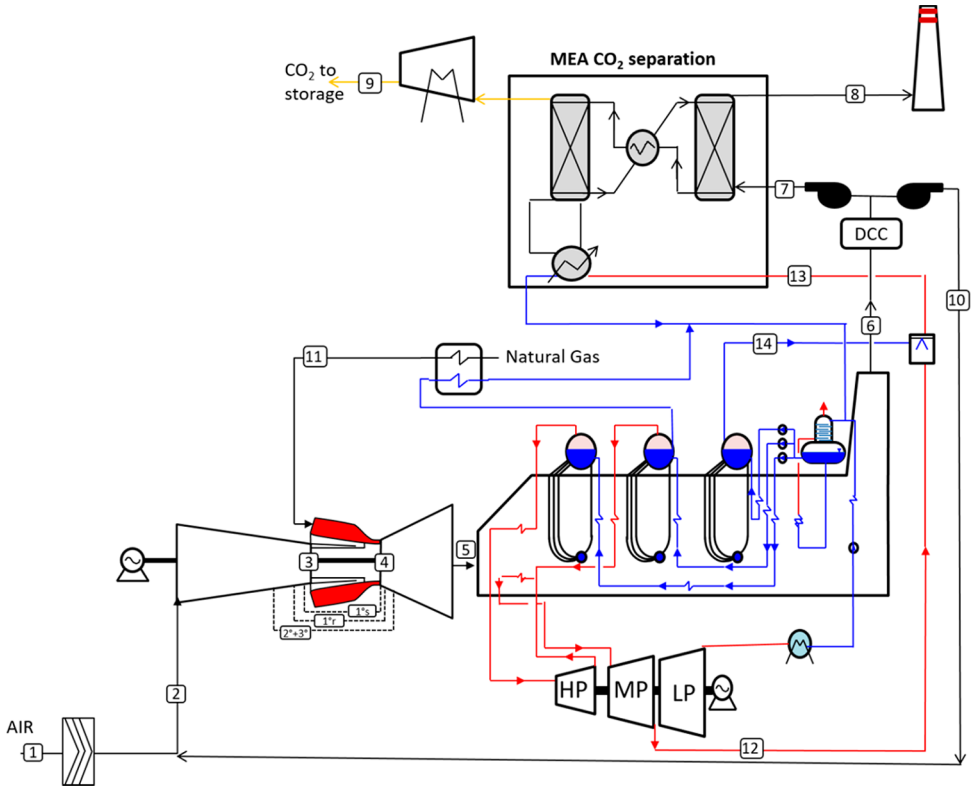

Figure 4. PFD of the CCGT MEA configuration with exhaust gas recycle.

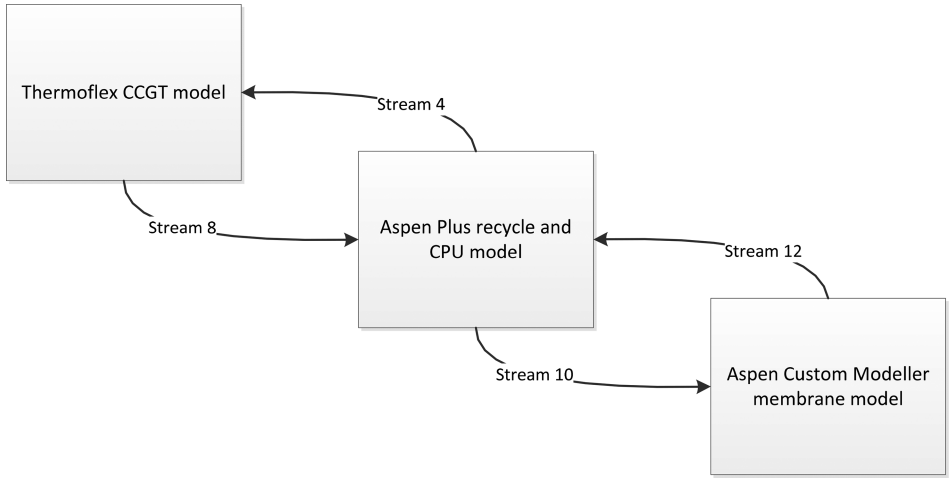

Figure 5. Representation of model linking. The Thermoflex model was used to simulate the CCGT performance; the Aspen Custom Modeler software, to simulate the membrane separation. Aspen Plus was used to model the exhaust gas recycle, including DCC and compressors, and CPU for the membrane case, as well as the MEA plant and CO_2 compressor in the MEA case.

models and software packages. These were soft-linked to simulate the total system. The mass balances were closed/converged manually, which required one, to several, iteration loops. The soft-linking of the models was, however, preferred over using one modeling language to describe all parts of the systems, because the selected models represent the state of the art of the technologies they describe, and already possessed the option of part load, or off design modeling. Thermoflex for instance includes performance maps of gas and steam turbines, allowing their part load assessment. Aspen Plus has the capability of rate-based column simulation and design, thus allowing the design and off design simulation of DCCs, absorbers, and strippers. Both software packages however exclude membrane models; hence Aspen Custom Modeler was selected to simulate this part. The use of already existing models in these different software packages was considered the most efficient way to simulate the total CCGT-SEGR-membrane and CCGT-EGR-MEA systems.

CCGT Modeling. The combined cycle power plant was modeled with Thermoflex V24.[32] The Thermoflex suite comprises numerous equipment that are used in power plants and allows easy convergence of thermal power cycles. It also contains a database of several hundreds of gas turbines, including their performance maps.

To model the reference CCGT according to the EBTF guidelines, the GE 9371F gas turbine was selected from the Thermoflex database (Table 2, Figure 5). This turbine was

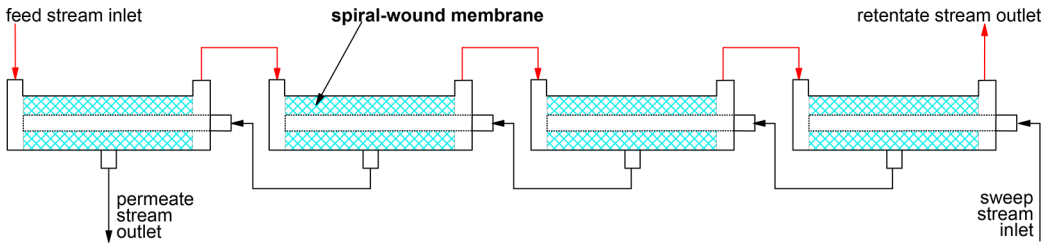

Figure 6. Spiral-wound membranes connected in series to produce a countercurrent flow. Reprinted from ref 15. Copyright 2017 Elsevier B. V.

chosen because the turbine outlet temperature (TOT; 646 °C) matched the temperature design of the EBTF HRSG (565 °C). The combined cycle was designed as a 2−2−1 configuration, meaning that two GTs were applied and two HRSGs fed into one steam turbine (ST) train. The CCGT was first modeled in the "engineering design" mode to estimate its thermodynamic performance and calculate the sizes of all equipment (pumps, heat exchangers, turbines, and cooling equipment). Then the thermodynamic performance at the selected part load operating points was simulated using the "off design" mode.

The selected GT model was also used to simulate the capture cases with EGR and SEGR. This means that it has a slightly different performance because the GE turbine is designed for operation with pure air as oxidant. The consequences of this choice will be discussed in Results and Discussion sections.

Membrane Modeling. The membranes (CCM and CRM) were modeled in Aspen Custom Modeler (ACM) using the model presented in ref 15. It was assumed that for both CCM and CRM spirally wound membranes were used because these tend to have a low pressure drop. In membrane design, countercurrent flow of feed gas and sweep gas (or permeate gas) achieves the most favorable partial pressure profiles and thus favorable driving force. Although the flow direction in spirally wound membranes is cross-flow, when placed behind each other in series, they mimic the behavior of a countercurrent flat plate (Figure 6). Therefore, the ACM model assumes countercurrent planar flow and divides the plate into k cells to calculate the species profiles over the membrane, with k set to 200 (Figure 7).

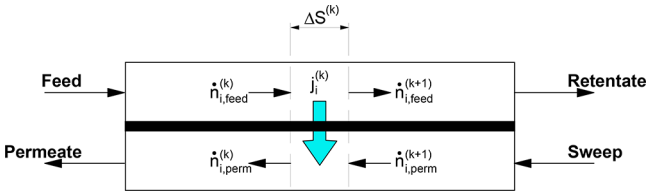

Figure 7. Axial discretization of the membrane model. Reprinted from ref 15. Copyright 2017 Elsevier B. V..

The mass flux through the membrane is described by eq 1, which relates the areal flux J_i (mol/m^{2}s) to the partial pressure difference of species i and the permeance of species i:

$$J_i = K_i(P_{\text{feed}}x_{i,\text{feed}} - P_{\text{perm}}x_{i,\text{perm}}) \quad (1)$$

where K_i is the permeance of species i; P is the total pressure at the feed and permeate sides; and x_i is the mole fraction of species i at feed and permeate sides (see Table 3 for membrane permeability and selectivities).

The mole balance (Figure 7) of each species and in each cell is described by

$$j_i^k = (\dot{n}_i^{(k-1)} - \dot{n}_i^k) \quad (2)$$

Table 3. Polaris Membrane Permeance [1 GPU = 10^{-6} cm^3(STP)/(cm^2 s cm$_{Hg}$)] and Selectivity.[34]

		selectivity of CO_2 with respect to			
membrane technology	permeance (GPU)	Ar	H_2O	N_2	O_2
Polaris	1000	5	0.3	50	5

where j_i^k is the molar species flux through the membrane (mol/s) and n is the molar flow (mol/s) into cells k and $k-1$, respectively, for each species i. Only species diffusion through the membrane is included in the mole balance; axial dispersion was assumed negligible.

Equation 3 links eqs 1 and 2 by multiplying the areal flux with the area of a cell:

$$j_i^k = J_i\Delta S_k \quad (3)$$

Finally, a variant of Fick's law of diffusion was used to describe the concentration gradient in the bulk phase of the gas flows (feed and permeate):[15,33]

$$J_i = \frac{(Sh)D_iP}{D_hRT}\ln\left(\frac{1 - x_{i,\text{bulk}}}{1 - x_{i,\text{interface}}}\right) \quad (4)$$

where Sh is the Sherwood number, D_i is the binary diffusion coefficient for species i, D_h is the hydraulic diameter (which is equal to twice the channel height), R is the gas constant, and T is the temperature.

The equations were solved with the finite difference method using the ACM DMO solver. For further details on the membrane model (including the thermal balance and the pressure drop calculation), the reader is kindly referred to ref 15.

The ACM membrane model was soft-linked with an Aspen Plus model (Figure 5) to simulate the DCC, compressors, and CPU, according to the specifications in Table 2. The Aspen Plus model was, in turn, soft-linked with the Thermoflex CCGT model (Figure 5). Because the three models were soft-linked, convergence of the selective exhaust gas cycle (stream 4; see Figure 5) was done manually, focusing on closing the mass balance of the total stream, as well as the species balances of CO_2 and O_2. The convergence allowed a maximum deviation in stream 4's total flue gas mass flow of 0.5% and a maximum error of 1% in the mole fractions of oxygen and carbon dioxide. The models were first run at full load to determine the required membrane areas and DCC column size. These sizes were then fixed (except for the CRM size; see Part Load Operation Strategies below) after which the models were run at the part load operating points. The oxygen concentration of the flue gas (GT exit) was always kept above 4.75% to ensure full fuel combustion.

MEA Modeling. The MEA unit was modeled in Aspen Plus using the e-NRTL thermodynamic model with symmetric

reference state. Gas phase behavior was predicted by the Redlich−Kwong equation of state. To analyze the capture plant performance at off design, a rate-based approach was used. To this end, the bicarbonate formation and the MEA carbamate formation reaction (eqs 4 and 5) rates were modeled using the Arrhenius formula (eq 6), applying the pre-exponential factors and activation energies provided by Kvamsdal and Rochelle.[35]

$$OH^- + CO_2 \rightarrow HCO_3^- \quad (5)$$

$$MEA + CO_2 + H_2O \rightarrow MEACOO^- + H_3O^+ \quad (6)$$

$$r = k_0 \exp\left[\frac{-E}{RT}\right] \quad (7)$$

where r is the reaction rate; k_0 is the pre-exponential factor; E is the activation energy; R is the gas constant; and T is the temperature. The other reactions in the H_2O-MEA-CO_2 system were modeled based on chemical equilibrium.

The MEA plant was first simulated at full load, in which the size of the columns was determined assuming a maximum flooding of 80%. Afterward, the column sizes were fixed and the model was run with the flue gas flows of the selected part load CCGT operating points. The MEA model was soft-linked with the flue gas flow from the CCGT HRSG, and with the IP/LP crossover steam, and condensate return. The pressure drop from the IP/LP crossover to the stripper reboiler was modeled using a duct containing four bends and a desuperheater in the Thermoflex software.

PART LOAD OPERATION STRATEGIES

CCGT. At part load, the gas turbine is operated such that it maintains the turbine outlet temperature, while producing the required GT set point power output. This strategy is maintained until the surge point of the GT air compressor. From this point onward only the fuel is reduced while keeping the air inflow constant. At lower GT loading the efficiency drastically drops, leading to a higher flue gas flow per produced MW of electricity. The significance of this will be further discussed in Results.

The steam cycle is controlled such that the feedwater mass flow reduces pro rato with the flue gas flow. To operate the steam turbine, their input volumetric flows need to remain constant, meaning that their input pressure is reduced at partial load. This operating philosophy is called sliding pressure control. The temperature settings of the steam cycle are kept constant over the entire loading range. This control strategy also implies that the pressure of the IP/LP crossover is reduced at partial load.

Membrane Plant. Part load operation of the membrane plant was at the core of this study: the starting point was that the energetic performance of membrane capture would improve at part load, due to the increasing specific surface area, and hence a decrease of the required externally imposed driving force, i.e., pressure ratio, would lead to a lower specific compression energy.

The membrane configuration allowed three different part load strategies (Table 4).

(1) Reduced Surface Area: A common practice in membrane operation is to reduce the surface area with decreasing feed flow.[36] Since membranes are modular devices, parallel modules can easily be taken offline. This strategy does not benefit from the increased surface area per cubic meter of feed flow during part load but rather provides a baseline for membrane performance at partial load. In this strategy, the pressure ratio over the membranes, as well as the CO_2 recovery, were kept constant.

Table 4. Membrane Operating Strategies at Part Load[a]

	variable area	variable back pressure	variable feed pressure
CCM area	free	fixed	fixed
CRM area	free	free	free
CCM recovery	fixed	fixed	fixed
CRM recovery	fixed	fixed	fixed
overall CO_2 capture (%)	90	90	90
feed pressure	fixed	fixed	free
back pressure	fixed	free	fixed
sweep flow ratio	free	free	free
CO_2 content recycle	free	free	free

[a]Note that for every strategy the sweep gas flow and the CRM area needed to be free variables to close the SEGR mass balance.

The membrane area was varied, and its value was determined by the model for each part load operating point.

(2) Reduced Back Pressure: A second strategy is to reduce the CCM back pressure at part load. It takes advantage of the larger specific surface area because the CO_2 vacuum pump consumes less energy per unit of captured CO_2. In this strategy, the feed pressure, CO_2 recovery, and CCM membrane area were fixed, while the CCM back pressure was a resulting variable.

(3) Reduced Feed Pressure: The third strategy impacts both CCM and CRM, by reducing the pressure of the feed flow at part load. The back pressure, capture rate, and CCM area were fixed, while the feed pressure was optimized. This strategy also has the potential of reduced specific compression energy at part load, due to the lower specific compression duty of the flue gas compressor.

In all three scenarios the CRM sweep gas was varied to close the mass balance over the NGCC-membrane recycle. Simultaneously, the CRM area needed to be varied to deal with changes in flue gas flow and composition. This was due to the nature of the membranes that also separate inert species at different rates during part load, as a result of the different operating conditions (pressure, flue gas flow, and so on). Also the oxygen concentration of the sweep gas to the GT was managed by varying the CRM surface area and sweep gas flow. The above description shows that the CCGT-SEGR-membrane cycle includes many variables that need to be controlled simultaneously, making control of such a system highly complex, especially during transients.

Last, the temperature of the cold box was adapted to deal with increasing shares of inerts that penetrated the CCM at part load. The resulting decrease in CO_2 mole fraction in the CCM permeate led to changed vapor liquid equilibria in the second cold box flash vessel, requiring more severe refrigeration to avoid venting large amounts of CO_2 with the inert gases.

MEA Plant. For the part load strategy of the MEA plant a fixed L/G ratio was assumed. This strategy is widely proposed as a suitable part load strategy by other researchers.[17,37−39] Sanchez Fernandez et al.[17] noted that when applying the fixed L/G strategy to a postcombustion amine unit integrated with a coal-fired power plant, the LP steam quality became insufficient at part load to maintain the L/G ratio constant. Their solutions were either to reduce stripper pressure in combination with constant L/G, thus allowing the stripper temperature to drop to values that sympathize with the lower pressure steam, or to increase the L/G ratio at lower loadings while keeping the stripper pressure constant, also accommodating the lower pressure reboiler steam. Other integrated studies, e.g., see

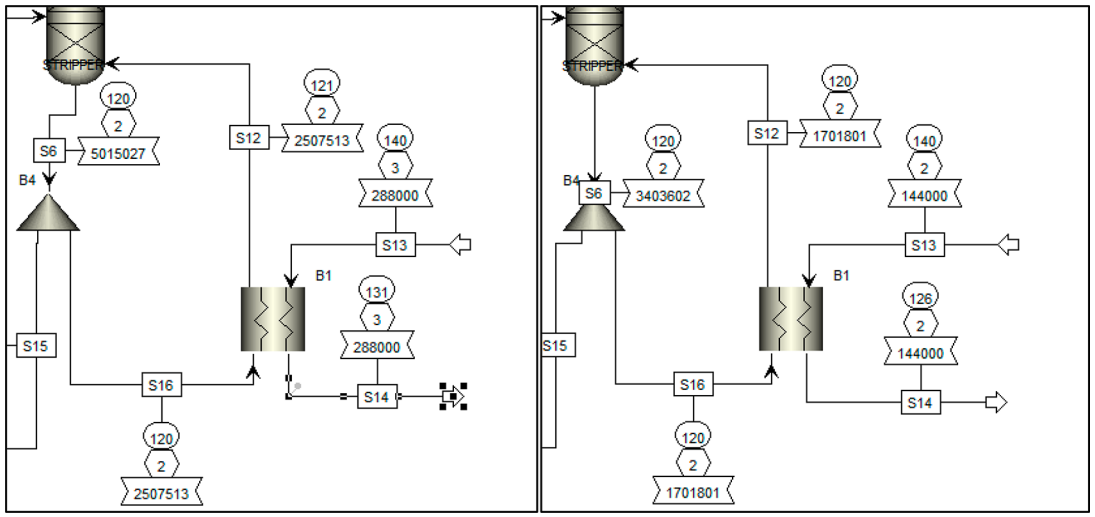

Figure 8. Screenshot of the stripper sump and reboiler model in Aspen Plus at the 100% (left) and 35% (right) GT load operating points. The values in the circles represent temperatures (°C), the hexagonal represents pressure (bar), and the flag-like boxes represent mass flows (kg/h).

Table 5. Overview of Capital Cost Items Included in This Study[a]

capital cost element to be quantified	name for sum of all preceding items	included in cost estimate
purchased equipment		√
supporting facilities (piping, instrumentation, etc.)		√
labor (direct and indirect)		√
	bare erected cost (BEC)	
engineering		√
procurement		√
construction		√
	engineering, procurement, and construction (EPC) cost	
contingencies		
process		
project		√
	total plant cost (TPC)	

[a]Table based on ref 40.

ref 37, do not mention issues matching LP steam quality with required reboiler temperature. Because it is a relevant issue, the match between LP steam quality and required reboiler temperature at constant L/G was checked at maximum and minimum GT load (100 and 35%) by explicitly modeling the reboiler and the steam quality supplied to the reboiler. This was done by taking the reboiler out of the Aspen Radfrac block as shown in Figure 8. The pressure and thus the dew point temperature of the LP steam were taken from the off design calculations of the CCGT model (off design IP/LP crossover pressure minus off design pressure drop in steam duct, desuperheater, and reboiler). The pressure drop over the steam extraction pipe was modeled in Thermoflex using the Fanning equation assuming a pipe of 76 m length with four long 90° bends; the pressure drop over the HXs (desuperheater and reboiler) was assumed to be 2% for each per the EBTF guidelines.[18]

Finally, two scenarios were modeled using the fixed L/G strategy: one baseline scenario where at every operating point 90% CO_2 was captured and one scenario where the capture gradually increased as the power plant loading decreased, from 90% capture, at 100% GT loading, to a maximum value of 96% CO_2 capture, at 35% GT loading. The latter scenario—the MEA 96% scenario—was meant to explore the possibility of increased CO_2 capture at lower loading, making use of the increased specific packing area per cubic meter of flue gas flow.

COST ESTIMATION

Capital Cost Estimates. The capital costs in this study were calculated as total plant costs (TPCs; Table 5), including purchased equipment costs, erection and installation, engineering, procurement and construction (EPC), and contingencies, following the common costing methodology for power and CCS technologies.[40] Owner's costs and interest during construction were excluded because they are highly location and owner specific and have limited added value for initial technology cost comparison. All capital costs are representative of an *N*th of a kind plant and were calculated as an AACE class 4 estimate, with an accuracy of −30% to +50%. The cost estimate represents a plant built in Rotterdam, The Netherlands, in 2015 €.

The capital costs of the CCGT equipment were calculated with the exponent method.[4,31] The gas turbine, steam turbine, HRSG, and heat rejection sections were scaled individually using the EBTF cost estimates[18,22] as a basis (Table 6). Based on DOE NETL,[41] an exponent of 0.7 was used for the HRSG and heat rejection equipment, and 0.8 for the gas and steam turbines. DOE NETL does provide even more detailed scaling factors, at a lower level of equipment aggregation, but in our experience the more detailed equipment scaling changes the capital costs by only single percentages, and hence the scaling of plant sections rather than individual equipment was found reasonable for the AACE class 4 estimate.

The capital costs of the (S)EGR and capture plant equipment were calculated using the bottom up, or factoring, approach.[31] To this end, the purchased equipment costs, installation costs, and EPC were calculated with the Aspen capital cost estimator V9.0 and multiplied with 40% project contingencies, corresponding to the AACE class 4 estimate.[40] Most equipment could be estimated using the Aspen capital cost estimator, except for the costs of the membranes and the costs of the large rotating equipment. Instead, membrane and rotating equipment costs were calculated using cost relations provided by Roussanaly et al.[16] (Table 6). We cross-checked Roussanaly's

Table 6. Cost Assumptions Used in This Study

Financial Assumptions			
real discount rate			7.5%
project lifetime			25 years
construction duration[a]			3 years
Capital Cost Relations for Power Plant Equipment			
	reference equipment, refs 18 and 22		
power plant section	EPC costs (M €$_{2008}$)	base size	exponent used[b]
gas turbine	189.22	544 MW	0.8
heat recovery steam generator	87.52	665.3 kg/s flue gas inflow	0.7
steam turbine	82.74	293 MW	0.8
heat rejection and miscellaneous	95.38	470 MW	0.7
Capital Cost Relations for Membranes and Large Rotating Equipment (Taken from Ref 16)			
equipment		bare erected cost relation (€$_{2014}$)	
vacuum pump		800 €/kW	
compressor (P_{out} = 1−4 bar)		920 €/kW	
compressor (P_{out} = 4−16 bar)		510 €/kW	
compressor (P_{out} > 16 bar)		370 €/kW	
membrane		40 €/m^2	
membrane housing[c]		$C = 286\left(\frac{A}{A_{ref}}\right)^{0.7}\left(\frac{P}{P_{ref}}\right)^{0.875}$	
Capital Costs of Other Equipment			
EPC costs of all other equipment (e.g., columns, packings, heat exchangers)		estimated using the Aspen capital cost estimating software V9.0	

[a]Included in project lifetime. [b]Based on ref 41. [c]The relation for the membrane housing cost was presented in ref 16 based on costs reported in ref 42. A and A_{ref} represent the membrane areas in this study and in the base case. P and P_{ref} represent the membrane feed pressures in this study and in the base case. The reference area is 2,000 m^2, and the reference pressure is 55 bar. The maximum area A for one membrane module is 25,000 m^2.

compressor cost figures with vendor quotes reported by Knoope et al.[43] and found them to compare satisfactorily. Note however, that industrial data on less common equipment such as large CO_2 capture membranes are scarce, and the costs reported in scientific literature need to be considered an indication rather than an absolute.

Operational Cost Estimates. The operational costs were calculated either as fixed, or as variable operating costs. The fixed costs were calculated as a fixed value per year, whereas the variable operating costs were estimated for each operating point specifically (from MSL to MCR), following the equations in Table 1. The variable operating costs of each operating point were subsequently added to the other yearly cash flows (Table 1).

The fixed operational cost estimates included labor and fixed maintenance and were calculated the same as in our previous work.[31] The consumables and waste disposal flows (kg/h) of the MEA plant were based on the full load flows reported in ref 31. They were subsequently calculated for each operating point by reducing them proportionally with the reduction in flue gas flow. The consumables and waste flows were then multiplied with their operating times (h/a (annum)) and with unit costs reported in ref 31, rendering the variable operational costs for each operating point (following the equations in Table 1).

A similar approach was followed to calculate the costs of membrane replacement. Many scholars report membrane replacement frequencies of 5 years when capture plants are run at full load (85% CF or 7446 h/a).[14,16,44] In this study, it was assumed that the replacement frequency increased with the time that the capture plant stands idle in the part load scenario. This led to a replacement frequency of 6 years instead of 5. This approach is crude, as is the approach used to calculate the MEA variable costs at part load. They are a first approximation given that phenomena such as MEA degradation and membrane degradation at part load are yet to be investigated.

Also, the costs of plant start-up and shutdown were added. Reported start-up costs are scarce because they are viewed as business sensitive information. Brouwer et al.[12] provided an overview of reported power plant start-up costs and suggested the values by Lew et al.[45] were the most reliable and inclusive. We adopted this suggestion and multiplied Lew's cost values with the number of hot, warm, and cold starts that a mid-merit gas power plant makes in a year (Table 7, retrieved from ref 37).

Table 7. Start-up Frequency and Costs[a]

	downtime prior to start (h)	no. of starts	start-up costs (€/MW$_{installed}$ per start)[b]
hot starts	<16	77	27
warm starts	16−64	63	39
cold starts	>64	17	57

[a]The number of starts is representative of a mid-merit CCGT.[37] [b]CCGT start-up costs according to the broad definition including maintenance and capital, forced outage, start-up fuel, and efficiency loss, reported by Lew et al.[45]

These start-up costs only apply to the CCGT plant. Start-up costs of MEA or membrane plants are yet to be reported but are expected to be smaller than those of the power plant, among others because less preheating is required.[12]

Last, the costs of CO_2 transport (6 €/tonne) and storage (10 €/tonne) were added, assuming 180 km transport to an offshore depleted oil or gas field, without the reuse of existing pipelines or production wells, similar to those in refs 4 and 31.

Note that reliable field, or industrial, data on many of the described operational costs are scarce in the public domain. Items such as solvent makeup in large demo or commercial scale capture plants have only recently been reported (e.g., see ref 46; some pilot results have however been published, e.g., see refs 47−49), and for instance the assumptions on membrane replacement are based on estimated guesses, rather than measured degradation rates. Also, the frequently reported costs of CO_2 capture membranes (40 €/m^2 or $50/m^2) are based on non-CO_2 capture industrial processes such as reverse osmosis and ammonia production (e.g., see refs 34 and 42) and are subsequently repeated by follow up studies (e.g., see refs 13, 14, and 16). Start-up costs of power plants are also notoriously hard to find, as described in ref 12. For the purpose of feasibility studies these caveats may be acceptable, because many operational costs are a small fraction of total costs, as we will show in

Results. But for a more detailed understanding of (power and) capture plant operations and costs, it is elementary that operational results from demo or commercial CCS plants become more widely available to the public.

Levelized Cost of Electricity. Finally, based on the technical performance and cost estimates, the part load LCOE was calculated using the equations in Table 1, assuming a 7.5% real discount rate[31] and a lifetime of 25 years including 3 years of construction[31] (Table 6).

RESULTS

This section describes the behavior and performance of the CCGT configurations. A selection of results will be presented, especially focusing on the behavior of the various parts of the studied configurations and their interfaces, and their impact on techno-economic performance. A complete list of technical performance results can be found in the Appendix.

Power Plant Behavior over Its Loading Range. Figure 9 presents the fuel input and exhaust flow of the gas turbine over its loading range. The fuel input declines (linearly) over the loading range, but the reduction is not proportional with the GT loading. For example, at 50% GT load, the fuel input is around 60% of the maximum. This is caused by the declining GT efficiency at partial load (Figure 10A); the GT runs at optimal efficiency at its design point, i.e., the max continuous rating (MCR). The GT gross efficiency declines from almost 38% at MCR to less than 26% at 35% loading. As a consequence, also the flue gas flow declines slower than the GT loading (Figure 9B and Figure 10C). This is relevant for the part load performance of the membrane configuration, as will be shown in the next section.

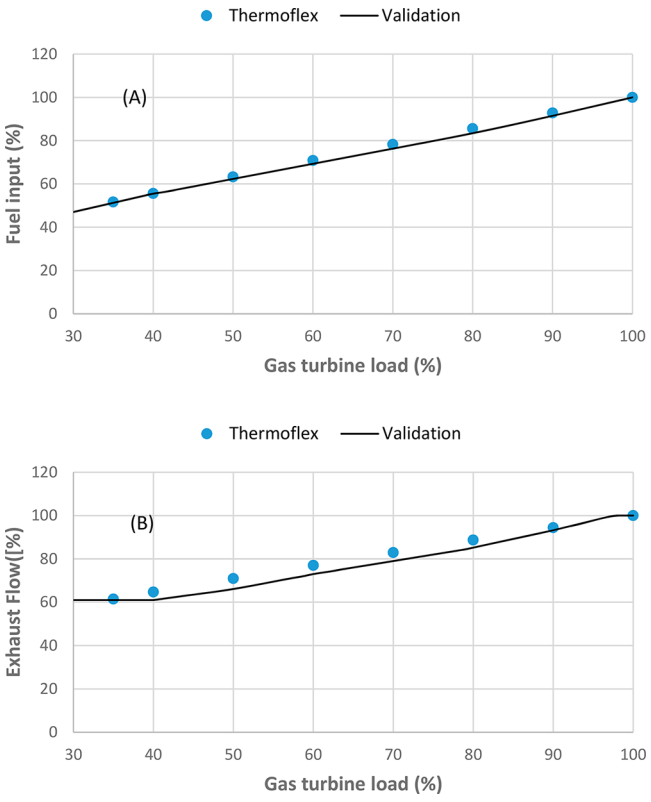

Figure 9. GT fuel input (A) and exhaust flow (B) as a function of GT loading. The blue dots represent the outputs of the Thermoflex GE 9371 FB gas turbine model. The black line represents measured operational data of a GE9351(FA) gas turbine as validation.

The Thermoflex model of the GE9371FB turbine compares well to measured operational GT data (see the black lines in Figure 9A,B). Note that operational plant data of the GE9371FB turbine were unavailable, so we used operational data from the GE9351(FA) gas turbine to validate the turbine model. The latter is also an F-class turbine that is used in combined cycles, with similar GT efficiency, pressure ratio, and turndown, but designed for a wider fuel range than that of the GE9371FB.

The GE9371FB efficiency drops significantly when (S)EGR is applied. With increasing CO_2 concentration in the oxidant stream, the GT gross efficiency decreases with as much as 3.5% point in the case of SEGR (Figure 10A). This is because the GT model aims to maintain the turbine outlet temperature constant, while the heat capacity of the NG/oxidant mixture changes with respect to the normal situation. This leads to a decrease in TIT and pressure ratio, and thus efficiency. The effect of this is presented in the next section, and further reflected upon in Discussion. Naturally, also the gross combined cycle efficiency of the CCGT membrane configuration is lower than that of the CCGT without CCS configuration (Figure 10B). Note that the gross efficiency of the CCGT MEA configuration is even lower due to steam extraction for the MEA reboiler. Last, also in the CCS cases, the flue gas flow declines linearly with GT loading (Figure 10C), but also not pro rato. The flue gas flow to the capture unit in the CCGT MEA configuration is lower over the whole loading range because of the recycling of flue gas to the GT.

Capture Technology Performance. *Membrane Plant Performance and Recycle Mass Balance.* The performance of the membranes at part load improved versus the performance at full load, confirming the starting hypothesis. Indeed, at part load it was possible to reduce either the membrane area, back pressure, or feed pressure while still capturing 90% of the CO_2. At part load, the flux was higher due to lower gas velocities over the membrane; however this applied to all the species, so also the inerts migrated more easily.

Another observation was that O_2 migrated through the CRM from the sweep gas (air) to the oxygen lean retentate (flue gas), because the O_2 partial pressure of the retentate was lower than that of the sweep gas. This caused the O_2 concentration in the oxidant flow (stream 3) to be around 13.5%$_{vol}$, rather than the 20%$_{vol}$ in normal air.

The increasing relative flue gas flow at partial GT loading caused a problem in the CRM-GT recycle mass balance: the sweep gas ratio needed to be increased with respect to the full load case, leading to a decline of the CO_2 concentration and an increase of the O_2 concentration in streams 3 and 4 (oxidant flow to GT compressor). As a result, for the variable area and variable back pressure strategy, it was not possible to close the mass and species balance at GT loadings smaller than 60% MCR, while maintaining high CO_2 concentrations of (close to) 20%$_{vol}$. In the variable feed pressure strategy, this did not occur: because of the lower pressure at the CRM feed side, the O_2 partial pressure of the retentate was lower, and more O_2 migrated from the permeate to the retentate side. This led to the same O_2 concentration being maintained of around 13.5%$_{vol}$ while allowing the CO_2 concentration to remain at levels above 18%$_{vol}$. To solve the species balance issue for the variable area and variable back pressure strategies, their feed pressure was also slightly reduced at GT loadings smaller than 60% MCR (see Figure 11A,B).

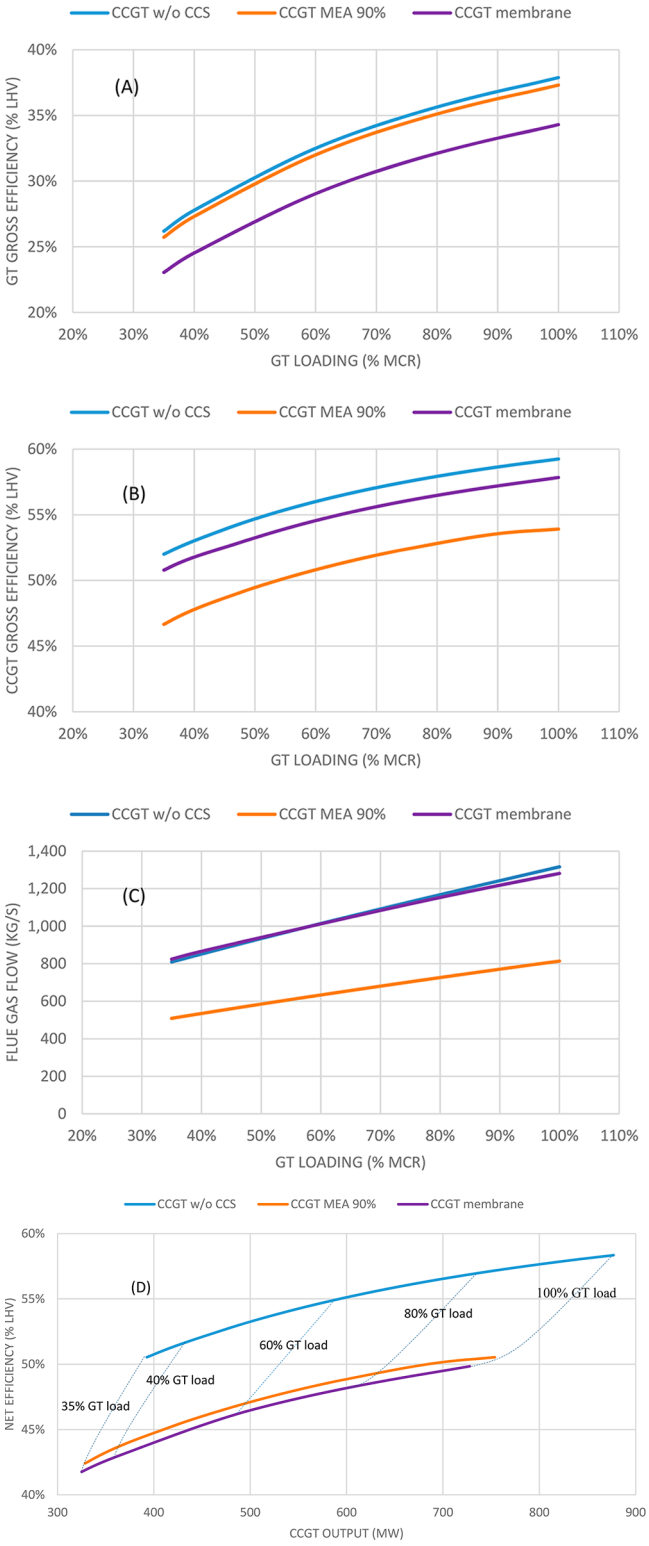

Figure 10. GT gross efficiency (A), CCGT gross efficiency (B), and flue gas flow (C) as a function of GT loading for the configurations without CCS, with MEA capturing 90% of the CO_2 at every operating point, and with membranes using the variable feed pressure strategy. (D) Net efficiency performance map of the three configurations as a function of the CCGT output.

The higher relative flue gas flow rate at part load also negatively affected the energy performance of the membrane configuration (see Appendix). The energy benefit of the reduced feed pressure in the variable feed pressure strategy was completely offset by

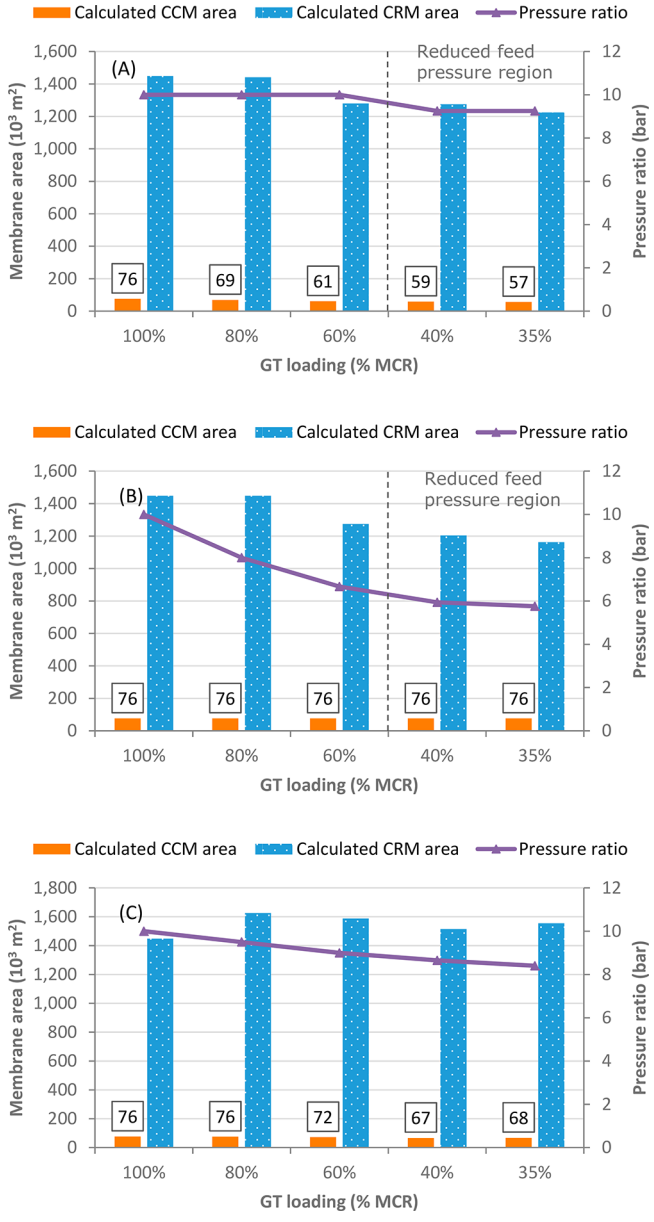

Figure 11. Calculated membrane area and pressure ratio over the CCM membrane. (A) Variable membrane area strategy, (B) variable back pressure strategy, and (C) variable feed pressure strategy.

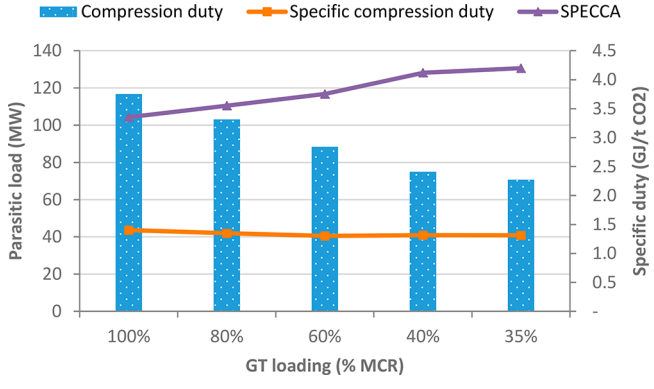

Figure 12. Energy performance of the membrane configuration with variable feed pressure over the GT loading range.

the additional compression power that the higher flue gas flow rate required (Figure 12). This negative effect was even larger

Table 8. IP-LP Crossover Pressure Levels, Reboiler Pressure, and Reboiler Temperatures over the Loading Range

	for given GT loading							
	100%	90%	80%	70%	60%	50%	40%	35%
IP-LP crossover pressure (bar)	3.52	3.39	3.27	3.15	2.99	2.85	2.72	2.58
reboiler pressure (bar)	3.35	3.23	3.13	3.02	2.87	2.74	2.63	2.49
condensation temperature (°C)	137.3	136.1	133.9	132.4	130.7	129.2	126.6	125.7
stripper temperature (°C, for fixed L/G)	120	120	120	120	120	120	120	120
available ΔT reboiler cold end (°C)	17.3	16.1	13.9	12.4	10.7	9.2	6.6	5.7

than the energy benefit for the variable back pressure strategy, leading to a higher total electricity use per CO_2 captured of the flue gas compressor than at 100% GT loading.

Of the three investigated membrane part load strategies, the variable feed pressure appears the most favorable, because the decrease in feed pressure led to the highest overall compression energy reduction. Despite the higher flue gas flow at part load, this strategy was able to maintain the same specific compression energy over the GT loading range (Figure 12). The SPECCA did increase significantly, such as for the MEA configuration, due to the reduction in CCGT efficiency at partial loading (Figure 12 and Figure 14). A drawback of the variable feed pressure strategy was that it required a higher CRM area at partial loading than at full load, thereby slightly increasing capital costs (next section).

MEA Plant and Steam Cycle–Reboiler Performance. As described in Part Load Operation Strategies (MEA Plant), the steam cycle pressure levels decline at lower loading; the IP-LP crossover pressure slowly reduces to 2.58 bar at MSL (Table 8). The modeled pressure drop in the reboiler steam pipe and HXs is however small, rendering usable steam condensation temperatures in the reboiler. Given the required solvent side reboiler temperature of 120 °C, the cold end of the reboiler still sees a 5.7 °C temperature difference when the GT is running at minimum load. The Aspen Plus model showed this is enough to operate the reboiler at part load (see Figure 8), given the large amount of exchanger area available relative to the solvent and steam flows. Although the log mean temperature difference decreased from 11 to 6.3 °C from maximum to minimum GT loading, the resulting *UA* (heat transfer) value stayed roughly the same at values of around 12 MJ/(s·K). This suggests that the fixed L/G strategy could be possible for part load operation of the CCGT MEA system.

Applying the fixed L/G strategy, the thermodynamic performance is stable over the GT loading range (Figure 13). The specific reboiler duty decreases with less than 0.1 point from full load to minimum load, indicating that the column design height already allowed CO_2 dissolution to approach equilibrium at full load. The SPECCA however increases at lower loading, due to the decreasing efficiency of the combined cycle (Table 1 and Figure 10D). The MEA 96% scenario led to lower CO_2 emission intensity than the MEA 90% scenario (Figure 14A). Because the additional energy requirement of the MEA 96% scenario was marginal (Appendix), this also led to a lower SPECCA than the MEA 90% scenario (Figure 14B).

Capital and Operational Cost Estimates. In addition to slightly better technical performance, the capital costs of the MEA configuration are also favorable over the membrane configuration (Table 9, −30%/+50% accuracy range, excluding owner's costs and interest during construction). This is partly due to the more expensive CCGT in the membrane configuration—the MEA configuration can do with a smaller,

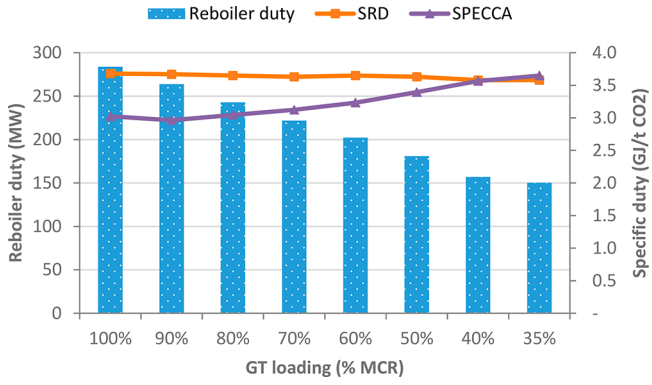

Figure 13. Energy performance of the MEA 90% scenario over the GT loading range.

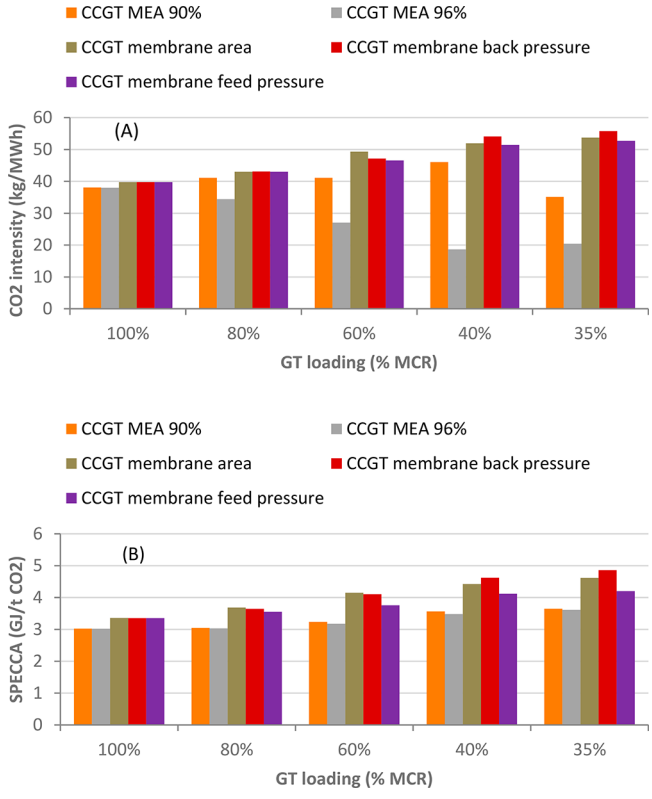

Figure 14. Technical performance of the five investigated CCGT with CCS configurations over the loading range of the GT. (A) CO_2 intensity and (B) specific primary energy consumption per tonne of CO_2 avoided.

hence cheaper, low pressure steam turbine—and partly due to the high costs of the recycle and membrane capture equipment. Also the CO_2 compression and purification section is much more expensive for the membrane configuration, owing to the

Table 9. Overview of Capital and Operational Costs of the Scenarios with and without CCS[a]

		CCGT MEA		CCGT membrane		
cost item	CCGT without CCS	90%	96%	area	back pressure	feed pressure
EPC costs (M€)						
CCGT	512	437	437	502	502	502
capture plant		249	249	338	338	346
compression plant/CPU (M€)		43	43	126	126	126
total EPC (M€)		729	729	966	966	974
total plant costs (M€)	564	889	889	1202	1202	1213
fuel costs (M€/year)	236	234	234	231	231	231
fixed operational costs (M€/year)	32	49	49	47	47	47
variable operational costs (M€/year)	3	9	9	3	3	3
membrane replacement costs (M€/(6 years))				76	76	85
transport and storage (M€/year)		24	25	24	24	24
restart costs (M€/year)	5	5	5	5	5	5

[a]The reported total plant costs inhabit a −30% to +50% accuracy range (AACE class 4 estimate). Note that MEA solvent replacement is included in the variable operational costs.

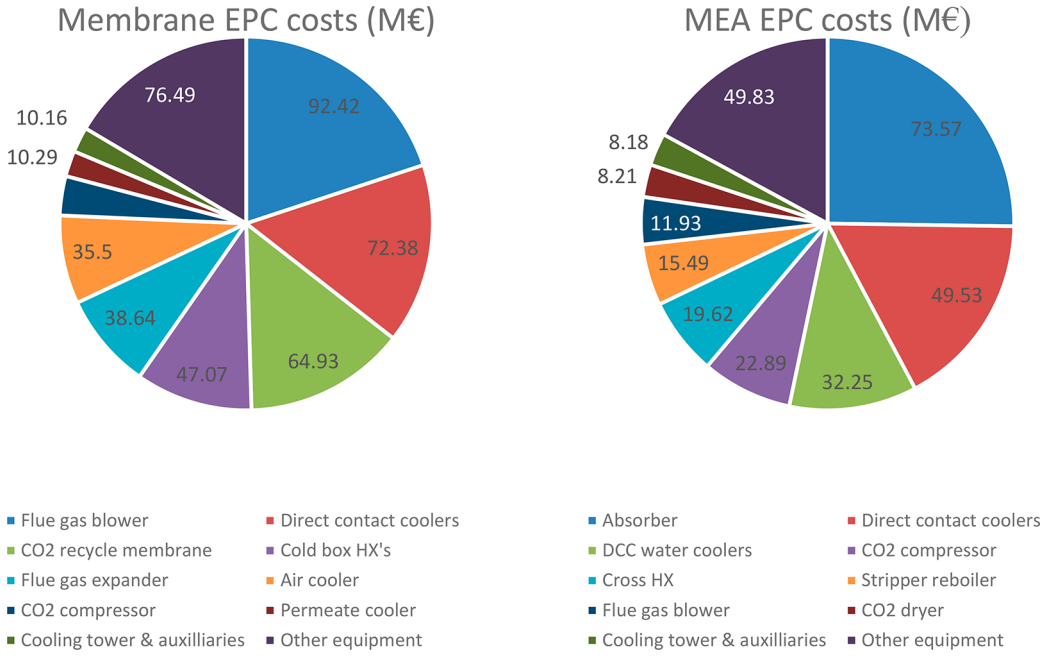

Figure 15. EPC breakdown for the membrane (left) and MEA (right) capture and compression plants (M€).

Table 10. Techno-economic Performance Indicators of the CCGT without CCS, with MEA Capture, and with Membrane Capture[a]

		CCGT MEA		CCGT membrane		
performance indicator	CCGT without CCS	90%	96%	area	back pressure	feed pressure
annual electricity output (GW h)	5229	4467	4455	4304	4299	4333
CO_2 emission intensity [kg/(MW h)]	378	40	29	47	47	46
SPECCA [GJ/(t of CO_2)]		3.3	3.2	3.9	4.0	3.8
total plant cost (M€)	564	889	889	1201	1201	1213
LCOE [€/(MW h)]	71.3	102.0	102.4	113.0	113.2	112.8
cost of CO_2 avoided [€/(t of CO_2)]		90.8	89.1	120.5	121.1	119.6

[a]Values are the weighted average values calculated over the power plant dispatch profile using the part load approach.

high costs of the cold box heat exchangers. The most expensive equipment of the membrane plant are the flue gas blower > direct contact coolers > CO_2 recycle membrane > cold box HXs > flue gas expander > air cooler (Figure 15). The other equipment have a smaller impact on the capital costs. The most expensive equipment of the MEA plant are absorber > direct contact coolers > DCC circulation water coolers > CO_2 compressor > lean/rich cross-HX > stripper reboiler (Figure 15).

The operational costs of the membrane configuration are some 10 M€/year lower than the MEA configuration; however, it suffers from a significant investment in new membranes every 6 years (Table 9). The restart costs are an order of magnitude smaller than the fixed operational costs and membrane replacement costs, and 2 orders of magnitude smaller than fuel costs, making their impact on lifetime costs minor. This applies to all configurations. Last, note that the transport and storage costs of

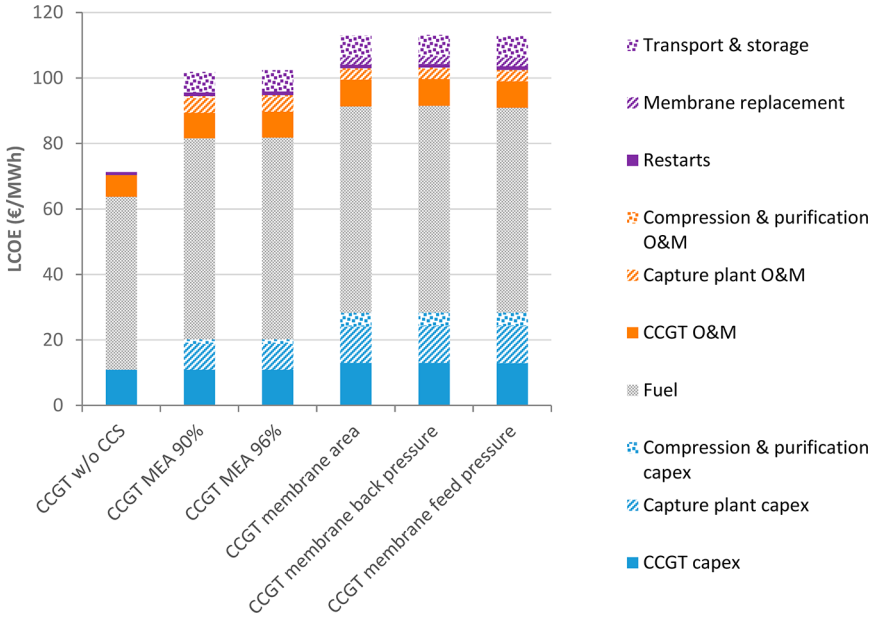

Figure 16. LCOE breakdown of the CCGT without CCS, with MEA capture, and with membrane capture. Values are the weighted average values calculated over the hypothetical power plant dispatch profile using the part load approach.

Table 11. Comparison of the Part Load LCOE (Based on the Hypothetical Dispatch Profile) and the Full Load Method (Assuming an 85% Capacity Factor)

		CCGT MEA		CCGT membrane		
performance indicator	CCGT without CCS	90%	96%	area	back pressure	feed pressure
part load LCOE [€/(MW h)]	71.3	102.0	102.4	113.0	113.2	112.8
full load LCOE [€/(MW h)]	64.8	90.9	90.9	98.8	98.8	98.8

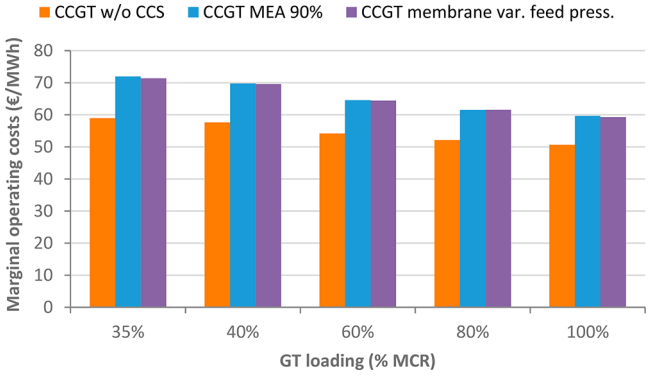

Figure 17. Marginal operating costs of the CCGT per operating point. The figure shows the case without CCS, with the 90% MEA capture scenario, and with membrane capture applying the variable feed pressure strategy.

the MEA 96% case are 1 M€/year higher than for the other cases, since a larger yearly amount of CO_2 is captured from the power plant.

Techno-economic Performance Indicators Using the Part Load Approach. Table 10 and Figure 16 present the techno-economic performance of the CCGT plant with and without CCS. It shows the weighted average performance of the CCGT configurations assuming the hypothetical dispatch profile that was the basis of this study (Figure 1), calculated using the part load approach (Table 1). Table 10 and Figure 16 allow easy insight into the performance of the investigated configurations relative to each other when investigated under the assumption of a realistic dispatch profile. They show the usefulness of the approach for R&D policy and decision making by capturing the complexities of flexible (real) dispatch in simple performance metrics.

Table 10 and Figure 16 show that the postcombustion MEA configuration is the more favorable CO_2 capture alternative, also when part load operation is taken into account. The MEA configuration clearly shows a lower emission intensity, a lower SPECCA, and lower costs than the membrane configuration. Of the two investigated MEA scenarios, the 96% capture scenario shows the lowest emission intensity, at comparable energy efficiency, and at comparable costs per megawatt hour as the 90% capture scenario. Of the membrane strategies, the reduced feed pressure strategy is the most favorable, presenting the best thermodynamic performance. The LCOE is, however, similar to the other membrane strategies due to the slightly higher membrane area (and thus costs). Furthermore, Figure 16 shows that the fuel costs make up the majority of the LCOE but that the higher capital and membrane replacement costs of the membrane configurations cause the LCOE difference with MEA. The power plant restart costs have a very limited impact on LCOE. As a reference, Table 11 compares the LCOE of all the configurations when calculated with the part load approach and when full load operation (85% CF) is assumed. The cost ranking between the configurations is the same using the part load or the full load approach. The absolute values are, however, noticeably higher when the part load approach is used.

Finally, Figure 17 shows the marginal operating costs of the CCGT per operating point, for cases without CCS, with MEA, and with membrane capture. The figure shows the expected result that the marginal costs are higher at lower loading, due to

Table 12. Techno-economic Performance of the CCGT without CCS, with MEA Capture, and with Membrane Capture, Assuming the Same GT Efficiency in the (S)EGR Cases as in Normal Operation[a]

		CCGT MEA		CCGT membrane		
performance indicator	CCGT without CCS	90%	96%	area	back pressure	feed pressure
CO_2 emission intensity [kg/(MW h)]	378	40	28	45	45	45
SPECCA [GJ/(t of CO_2)]		3.2	3.1	3.2	3.3	3.0
LCOE [€/(MW h)]	71.3	101.4	101.4	108.5	108.6	108.3
cost of CO_2 avoided [€/(t of CO_2)]		83.7	80.9	106.3	106.6	105.7

[a]Values are the weighted average values calculated over the power plant dispatch profile using the part load approach.

Table 13. Comparison of Results with Other Membrane/SEGR Studies

			this work	
	Turi et al.[15]	Merkel et al.[13]	no impact (S)EGR on GT efficiency	GT efficiency reduction due to (S)EGR
results calculated assuming	full load	full load	loading profile	loading profile
EGR used for MEA?	no	no	yes	yes
capital cost calculation MEA	reference used	reference used	own calculation	own calculation
capital cost calculation membranes	own calculation	own calculation	own calculation	own calculation
highest net system efficiency	membranes	membranes	depends on membrane part load strategy	MEA
lowest SPECCA	membranes	not available	depends on membrane part load strategy	MEA
lowest CAPEX	MEA	membranes	MEA	MEA
lowest LCOE	MEA	membranes	MEA	MEA

the lower efficiency of the CCGT cycles, and thus higher NG requirement per additional megawatt hour of power produced. The marginal operating costs are almost completely dictated by NG costs, and therefore the marginal costs of the MEA and membrane systems are very comparable. The MEA marginal costs are less than a single percentage higher due to the variable costs of operating the MEA unit (e.g., solvent makeup), which the membrane configuration does not incur. Therefore, from the perspective of marginal costs and merit order, the two CO_2 capture configurations perform very similarly.

DISCUSSION

Effect of EGR on GT Performance. In Results we discussed the reduced GT efficiency in the case of (S)EGR, which impacts the thermodynamic performance of the CCGT configurations with MEA and membranes. If exhaust gas recycles become more common, it is plausible that GT vendors will redesign GTs to improve their performance under conditions of higher CO_2 and lower nitrogen and oxygen concentrations. We studied this effect by assuming that the GT gross efficiency in the (S)EGR configurations is equal to that of combustion with normal air. The techno-economic performance indicators under this assumption are presented in Table 12. The improved GT efficiency significantly improves the technical performance of the membrane configurations: their SPECCA is reduced by ~0.75 GJ/(t of CO_2). The SPECCA of the MEA configurations improves less: ~0.1 GJ/(t of CO_2). This indicates that the membrane configuration could be technically competitive with MEA, if the GTs can be modified to run more efficiently on an (S)EGR oxidant composition. The LCOE and CCA of the membrane configurations are, however, still higher than that of MEA, owing to the high capital costs and membrane replacement costs. This implies that even with improved GT efficiency, the membrane system in this case study is unlikely to become economically competitive with postcombustion MEA solvent.

Impact of LP Steam Quality for Reboiler. Another issue that can favor the technical performance of the membrane configuration is the quality of the LP steam that is available for the MEA reboiler. Our modeling results showed that it is possible that the quality is sufficient to maintain the reboiler temperature around 120 °C without reducing stripper pressure, thereby allowing one to use a fixed L/G ratio at part load. The sufficient steam quality was a result of the low (modeled) pressure drop in the LP steam extraction pipe, desuperheater, and reboiler of around 0.1 bar. Sanchez-Fernandez et al.,[17] however, found pressure drops of up to 1 bar for the steam extraction pipe and heat exchangers, which negatively impacted the performance of their MEA model at part load. This could imply that our results are biased toward favorable MEA performance, and in a real plant the MEA and membrane technical performance could be more equal. Confirmation of either result can only be done in large demonstration or industrial size plants.

Comparison to Other Studies. Comparison of our results with the two other studies that investigated the membrane-SEGR cycle—only at full load—renders a mixed picture (Table 13). Turi et al.[15] confirm our results that membranes may have favorable technical performance over MEA, if the GT efficiency in the SEGR cycle is not impacted by differences in oxidant composition. They also confirm our findings that despite this, the Polaris membrane-SEGR cycle is not economically competitive with MEA. Merkel et al.[13] estimated that the membrane-SEGR cycle is also economically competitive with MEA. Note however that both studies did not use exhaust gas recycle in the MEA case, and did not calculate the MEA capital costs themselves, but rather used generic reference values. This means the assessment of the MEA and membrane configurations in those studies were not like-for-like, which may have impacted their results in favor of the membrane configuration.

Impact of Membrane Costs. As indicated in the description of the economic methods and results, the costs of commercial CO_2 capture membranes are still uncertain and may change the costs of electricity of the SEGR membrane system. Table 14 shows the change in LCOE when the membrane costs decrease with 50% or increase with 100% from the base value of 40 €/m^2 (Table 6). The impact of the membrane costs is limited for this system: cutting membrane

Table 14. Sensitivity of LCOE of Changes in Membrane Costs for the Variable Feed Pressure Part Load Strategy

	membrane costs		
performance indicator	low (20 €/m^2)	base (40 €/m^2)	high (80 €/m^2)
LCOE [€/(MW h)	110.1	112.8	118.1

costs in half reduces the LCOE with 3 €/(MW h), while a doubling in membrane costs increases the LCOE with 5 €/(MW h). The sensitivity of our system to membrane costs is more limited than the system earlier assessed by Turi et al.[15] This is explained by the higher dominance of fuel costs in our study—due to a higher fuel price assumption but also because Turi et al. assume a membrane replacement frequency of 3 years, rather than the 6 years in our study. This shows that higher membrane production costs may be allowed, if this significantly increases its durability.

Impact of Dispatch Profile. The selection of a dispatch profile can have a large influence on technology comparison if the performance δ of the technologies changes over the loading range. As discussed in Results, the relative performance difference between the MEA and the membrane configuration remains constant over the loading range, leading the overall conclusions on techno-economic performance to remain the same, despite the selected dispatch profile (Figure 18).

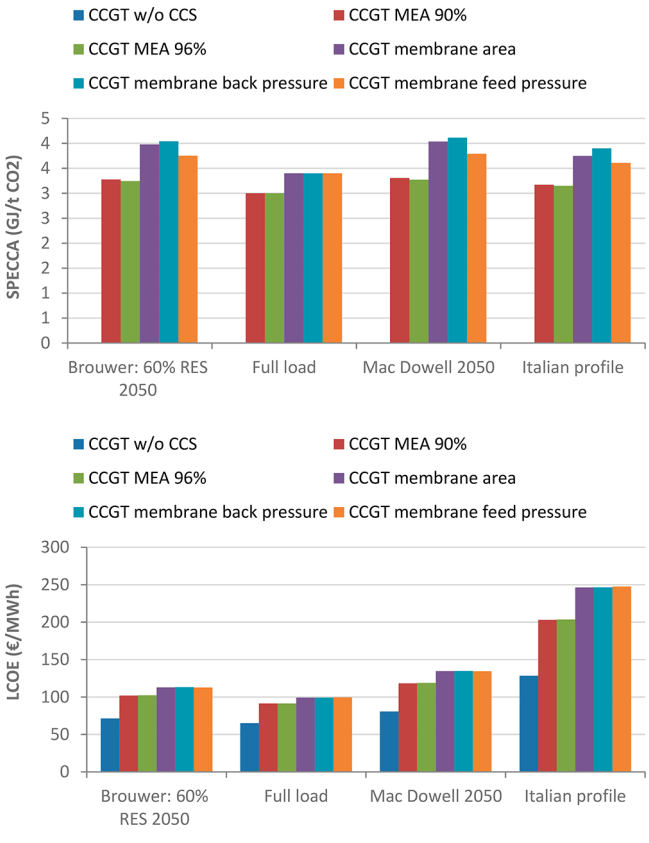

Figure 18. Techno-economic performance of the CCGT without CCS, with MEA capture, and with membrane capture, at different dispatch profiles. Values are the weighted average values calculated over the power plant dispatch profile. The Brouwer 60% RES 2050 profile was the hypothetical profile used as the basis of this study.

There are however noticeable changes in absolute values. Not surprisingly, the SPECCA and LCOE values are lowest in the profiles that lean toward full dispatch and are highest in the profiles that go toward minimal dispatch, stressing the relevance of including flexible operation and lower power with CCS plant utilization scenarios in techno-economic studies.

Operability of the SEGR-Membrane Configuration. Last, the results discussed the part load operation of the configuration with membranes and selective EGR and showed that part load operation required careful balancing of operational parameters to reach convergence while maintaining a high CO_2 content in the flue gas. Simultaneous varying of feed pressure, CCM and CRM surface area, and recycle flow appeared necessary. This suggests that the membrane confgiuration requires an advanced control scheme if it were to be built and that it is likely more difficult than MEA to operate optimally. We draw from this that although the SEGR cycle may look promising on the drawing board, real plants may better use normal EGR with MEA, or for instance with a simple membrane configuration (e.g., see refs 14, 16, 42, 44, and 50), unless membrane selectivity of CO_2 over N_2 but also O_2 can be significantly improved. As an indication, at membrane permeance of around 1000 gpu, a 10-fold increase of CO_2 selectivity to both nitrogen and oxygen (as used in this study, Table 3) would significantly improve the efficiency of the CCGT SEGR membrane system and is expected to also improve its operating stability.[15]

CONCLUSION

This work compared the techno-economic performance of a CCGT equipped with CO_2 capture using an advanced membrane configuration with selective exhaust gas recycle, and using MEA solvent, under the assumption of flexible power plant dispatch. This was the first time that the techno-economic performance of CO_2 capture technologies was compared assuming a flexible dispatch profile, and the assessment was done using a comprehensive, new, part load assessment method.

This work started from the hypothesis that the relative energy performance of postcombustion membranes versus postcombustion solvents improves at part load due to increased species flux through the membrane and resulting lower compression requirements. Our part load assessment method disproved this hypothesis: indeed at part load a higher species flux was observed—for all species—meaning that the pressure ratio over the membrane could be reduced, leading to lower energy requirements of rotating equipment. However, this reduction was offset because at part load the flue gas flow to GT output ratio increased, requiring relatively more flue gas to be compressed.

The part load method further highlighted that not only the membrane selectivity of CO_2 to N_2 is important but also the CO_2 over oxygen selectivity of the CO_2 recycle membrane should be significantly improved with respect to current performance. This would provide the plant operator with an essential means to control the gas composition of the exhaust gas recycle, without which it would be likely impossible to manage the plant through transients.

In this particular case, the conclusions on competitiveness of the assessed technologies are the same when analyzed at full load and at part load, because the technical performance δ between the technologies remained the same over the power plant loading range. The technical performance of the MEA configuration outperformed the membrane configuration over the whole CCGT loading range. The MEA SPECCA increased from 3.02 GJ/(t of CO_2), at 100% GT loading, to 3.65 GJ/(t of CO_2) at 35% GT loading; the membrane SPECCA using the most favorable part load strategy increased from 3.35 to

4.20 GJ/(t of CO_2) over the same loading range. The main reason for the lesser technical performance of the membrane configuration lies in the reduced gas turbine efficiency, due to the high CO_2 concentration caused by the selective recycling of CO_2 to the combustor. The picture changed if equal GT efficiency was assumed for combustion with normal air and with the SEGR oxidant. In that case the membranes' technical performance was comparable to that of MEA. The capital costs of the CCGT with membrane configuration were 35% higher than the CCGT with MEA configuration. That, and the 6 year replacement frequency of the membranes, led the part load levelized cost of electricity to be 112.8 €/(MW h) for the membrane, versus 102 €/(MW h) for the MEA configuration. The full load LCOE for the membrane and MEA configuration were 99.7 and 91.3 €/(MW h), respectively, significantly lower than the part load LCOE's. Only in terms of marginal operating costs, the membrane system performs on par with the MEA system. Furthermore, improving the GT efficiency for SEGR/membranes improved the LCOE of the membrane configuration, but not enough to become economically competitive with MEA.

The study further found that the LCOE difference between the membrane and MEA configuration becomes larger when lower dispatch is assumed, because the high capital costs of the membrane configuration start to weigh on LCOE more heavily at low plant utilization. Also, for technologies that show a distinctively different performance δ over the loading range (between maximum continuous rating and minimum stable load), the choice of dispatch profile becomes more relevant, and may favor one technology over another. Selection of a representative dispatch profile thus remains key to CCS technology comparison.

Finally, it should be noted that detailed techno-economic performance data are still lacking in the public domain, more so for membranes than for MEA. Examples are measurements of solvent make up in commercial solvent plants or the pressure drop between IP/LP crossover and MEA reboiler, and the effect of flexible operation on those. For the membranes, the most important caveat is on (the effect of flexible operation on) membrane replacement frequency. Also cost data are often scarce and/or have a weak knowledge basis. These gaps may not significantly change the results of early techno-economic feasibility studies (equivalent to AACE class 4), because at those levels one is interested in differences in the order of magnitude. The data gaps do become relevant when more detailed technology assessments are undertaken. Most of the missing information is of the operational kind and can thus only be made available by sharing results of extended trials in large demonstration or commercial size plants.

Concluding, the results in this study showed the importance of part load assessment of power plants and CCS technologies. Not only do they show that levelized electricity costs are higher in reality than in the full load studies but also part load assessment does provide critical insights into technology performance at off design conditions and the resulting effect on economics. This work showed that each investigated technology, NGCC, MEA plant, and membrane plant, responds differently to off design conditions, leading to relevant changes in part load performance. This knowledge is elemental not only for decision making on technology R&D and investment in new plants but also for technology comparisons, because one technology may be better suited to operate under realistic dispatch conditions than the other.

APPENDIX

Table 16 provides a breakdown of thermodynamic performance of the studied CCGT configurations.

Table 16

	for given GT load				
operating point	100%	80%	60%	40%	35%
CCGT					
fuel input (MW_{LHV})	1503	1287	1065	836	777
GT gross power output (MW)	570	459	346	233	204
ST gross power output (MW)	321	287	250	211	200
parasitic load (MW)					
power section	14	13	12	12	11
net power output (MW)	877	733	584	432	393
gross efficiency ($\%_{LHV}$)	59.24	57.92	56.00	53.02	52.00
net efficiency ($\%_{LHV}$)	58.35	56.93	54.86	51.63	50.53
CO_2 emission intensity [kg/(MW h)]	354	363	377	400	409
CCGT MEA 90%					
fuel input (MW_{LHV})	1492	1279	1060	833	775
gross power output (MW)	804	675	539	398	361
parasitic load (MW)					
power section	14	13	12	11	11
MEA plant	13	12	11	9	9
compression section	23	20	17	13	13
net power output (MW)	754	630	499	364	329
gross efficiency ($\%_{LHV}$)	53.91	52.82	50.81	47.79	46.66
net efficiency ($\%_{LHV}$)	50.53	49.29	47.08	43.71	42.41
CO_2 recovery (%)	90	90	90	90	93
CO_2 emission intensity [kg/(MW h)]	38	41	41	46	35
specific reboiler duty [GJ/(t of CO_2)]	3.68	3.65	3.65	3.58	3.58
SPECCA [GJ/(t of CO_2)]	3.02	3.05	3.23	3.57	3.65

Table 16. continued

operating point	for given GT load				
	100%	80%	60%	40%	35%
CCGT MEA 96%					
fuel input (MW_{LHV})	1492	1279	1060	833	775
gross power output (MW)	804	674	537	396	360
parasitic load (MW)					
power section	14	13	12	11	11
MEA plant	13	12	11	9	9
compression section	23	20	17	14	13
net power output (MW)	754	629	497	361	327
gross efficiency ($\%_{LHV}$)	53.91	52.74	50.71	47.56	46.51
net efficiency ($\%_{LHV}$)	50.53	49.19	46.91	43.37	42.21
CO_2 recovery (%)	90	92	94	96	96
CO_2 emission intensity [kg/(MW h)]	38	34	27	19	20
specific reboiler duty [GJ/(t of CO_2)]	3.68	3.69	3.65	3.63	3.63
SPECCA [GJ/(t of CO_2)]	3.02	3.03	3.18	3.48	3.62
CCGT membrane variable area					
fuel input (MW_{LHV})	1460	1257	1050	835	780
gross power output (MW)	845	710	573	432	396
parasitic load (MW)					
power section	15	15	15	15	15
membrane plant	57	52	46	35	34
compression and purification unit	44	40	35	29	28
net power output (MW)	728	603	477	353	320
gross efficiency ($\%_{LHV}$)	57.84	56.48	54.56	51.78	50.79
net efficiency ($\%_{LHV}$)	49.84	47.99	45.45	42.29	41.08
CO_2 recovery (%)	90	90	90	90	90
CO_2 emission intensity [kg/(MW h)]	40	43	49	52	54
SPECCA [GJ/(t of CO_2)]	3.35	3.69	4.15	4.42	4.62
CCGT membrane var. back pressure					
fuel input (MW_{LHV})	1460	1257	1050	835	780
gross power output (MW)	845	710	573	432	396
parasitic load (MW)					
power section	15	15	15	15	15
membrane plant	57	52	46	35	34
compression and purification unit	44	38	34	30	29
net power output (MW)	728	604	478	351	318
gross efficiency ($\%_{LHV}$)	57.8	56.5	54.6	51.8	50.8
net efficiency ($\%_{LHV}$)	49.8	48.1	45.5	42.0	40.7
CO_2 recovery (%)	90	90	90	90	90
CO_2 emission intensity [kg/(MW h)]	40	43	47	54	56
SPECCA [GJ/(t of CO_2)]	3.35	3.64	4.10	4.62	4.86
CCGT membrane var. feed pressure					
fuel input (MW_{LHV})	1460	1257	1050	834	778
gross power output (MW)	845	710	573	432	396
parasitic load (MW)					
power section	15	15	15	15	15
membrane plant	57	48	39	31	28
compression and purification unit	44	40	35	29	28
net power output (MW)	728	606	485	357	325
gross efficiency ($\%_{LHV}$)	57.84	56.48	54.57	51.80	50.86
net efficiency ($\%_{LHV}$)	49.84	48.26	46.15	42.81	41.76
CO_2 recovery (%)	90	90	90	90	90
CO_2 emission intensity [kg/(MW h)]	40	43	47	51	53
SPECCA [GJ/(t of CO_2)]	3.35	3.55	3.75	4.12	4.20

AUTHOR INFORMATION

Corresponding Author

*E-mail: vandersm@ipe.mavt.ethz.ch.

ORCID

Mijndert van der Spek: 0000-0002-3365-2289

Funding

This work was supported by the Norwegian Research Council under Project No. 218952 and by an industrial consortium (Bharat Petroleum, Uniper, and Norske Shell).

Notes

The authors declare no competing financial interest.

ABBREVIATIONS

AACE = Association for the Advancement of Cost Engineering
ACM = Aspen Custom Modeler
CCA = cost of CO_2 avoided
CCC = cost of CO_2 captured
CCGT = combined cycle gas turbine
CCM = CO_2 capture membrane
CCS = CO_2 capture and storage
CF = capacity factor
CPU = compression and purification unit
CRM = CO_2 recycle membrane
DCC = direct contact cooler
DOE = U.S. Department of Energy
EBTF = European Benchmarking Task Force
EGR = exhaust gas recycle
EPC = engineering, procurement, and contracting
GT = gas turbine
HRSG = heat recovery steam generator
IP = intermediate pressure
LCOE = levelized cost of electricity
L/G = liquid over gas
LP = low pressure
MCR = maximum continuous rating
MEA = monoethanolamine
MSL = minimum stable load
NETL = U.S. National Energy Technology Laboratory NG = natural gas
SEGR = selective exhaust gas recycle
SPECCA = specific primary energy per tonne of CO_2 avoided
SRD = specific reboiler duty
ST = steam turbine
TIT = turbine inlet temperature
TOT = turbine outlet temperature
TPC = total plant cost

REFERENCES

(1) NETL; Fout, T.; ESPA; Zoelle, A.; Keairns, D.; Turner, M.; Woods, M.; Kuehn, N.; Shah, V.; Chou, V.; Pinkerton, L. *Cost and Performance Baseline for Fossil Energy Plants Volume 1a: Bituminous Coal (PC) and Natural Gas to Electricity Revision 3*, DOE/NETL-2016/1723; National Energy Technology Laboratory (NETL): Pittsburgh, PA, USA, 2015.

(2) ZEP. *The Costs of CO_2 Capture: Post-demonstration CCS in the EU*; European Technology Platform for Zero Emission Fossil Fuel Plants: Brussels, Belgium, 2011.

(3) IEAGHG. *Water Usage and Loss Analysis of Bituminous Coal Fired Power Plants with CO_2 Capture*, Report 2010/05; International Energy Agency Greenhouse Gas R&D Programme (IEAGHG): Stoke Orchard, U.K., 2010.

(4) van der Spek, M.; Sanchez Fernandez, E.; Eldrup, N. H.; Skagestad, R.; Ramirez, A.; Faaij, A. Unravelling uncertainty and variability in early stage techno-economic assessments of carbon capture technologies,. *Int. J. Greenhouse Gas Control* **2017**, *56*, 221−236.

(5) van der Spek, M.; Manzolini, G.; Ramirez, A. New approach to techno-economic assessment of power plants with carbon capture and storage. The inclusion of realistic dispatch profiles to calculate techno-economics of part load operations.,. *Energy Fuels* **2017**, *31*, 1047−1049.

(6) Brouwer, A. S.; Van den Broek, M.; Seebregts, A.; Faaij, A. Impacts of large-scale Intermittent Renewable Energy Sources on electricity systems, and how these can be modeled,. *Renewable Sustainable Energy Rev.* **2014**, *33*, 443−466.

(7) Van der Wijk, P. C.; et al. Benefits of coal-fired power generation with flexible CCS in a future northwest European power system with large scale wind power,. *Int. J. Greenhouse Gas Control* **2014**, *28*, 216−233.

(8) Mac Dowell, N.; Staffell, I. The role of flexible CCS in the UK's future energy system,. *Int. J. Greenhouse Gas Control* **2016**, *48*, 327−344.

(9) Rubin, E. S.; Rao, A. B. Uncertainties in CO2 Capture and Sequestration Costs,. *Greenh. Gas Control Technol. - 6th Int. Conf.* **2003**, *II*, 1119−1124.

(10) Rubin, E. S.; Chen, C.; Rao, A. B. Cost and performance of fossil fuel power plants with CO2 capture and storage,. *Energy Policy* **2007**, *35*, 4444−4454.

(11) ENTSOE. Information on national generating capcities and national/European energy balances, *ENTSOE Transparancy Platform*, 2015. [Online]. Available: https://transparency.entsoe.eu/. [Accessed Aug. 5, 2016].

(12) Brouwer, A. S.; Van den Broek, M.; Seebregts, A.; Faaij, A. Operational flexibility and economics of power plants in future low-carbon power systems,. *Appl. Energy* **2015**, *156*, 107−128.

(13) Merkel, T. C.; Wei, X.; He, Z.; White, L. S.; Wijmans, J. G.; Baker, R. W. Selective Exhaust Gas Recycle with Membranes for CO 2 Capture from Natural Gas Combined Cycle Power Plants,. *Ind. Eng. Chem. Res.* **2013**, *52*, 1150−1159.

(14) Zhai, H.; Rubin, E. S. Techno-economic assessment of polymer membrane systems for postcombustion carbon capture at coal-fired power plants.,. *Environ. Sci. Technol.* **2013**, *47*, 3006−14.

(15) Turi, D. M.; Ho, M.; Ferrari, M. C.; Chiesa, P.; Wiley, D. E.; Romano, M. C. CO_2 capture from natural gas combined cycles by CO_2 selective membranes,. *Int. J. Greenhouse Gas Control* **2017**, *61*, 168−183.

(16) Roussanaly, S.; Anantharaman, R.; Lindqvist, K.; Zhai, H.; Rubin, E. Membrane properties required for post-combustion CO2 capture at coal-fired power plants,. *J. Membr. Sci.* **2016**, *511*, 250−264.

(17) Sanchez Fernandez, E.; et al. Operational flexibility options in power plants with integrated post-combustion capture,. *Int. J. Greenhouse Gas Control* **2016**, *48*, 275−289.

(18) *D2.4.3 European Best Practice Guidelines for Assessment of CO_2 Capture Technologies*, CESAR D2.4.3; CESAR Enhanced Separation & Recovery: Delft, The Netherlands, 2011.

(19) IEAGHG. *CO_2 capture at coal based power and hydrogen plants*, Report 2014/3; International Energy Agency Greenhouse Gas R&D Programme (IEAGHG): Stoke Orchard, U.K., 2014.

(20) Brouwer, A. S.; Van den Broek, M.; Zappa, W.; Turkenburg, W. C.; Faaij, A. Least-cost options for integrating intermittent renewables in low-carbon power systems,. *Appl. Energy* **2016**, *161*, 48−74.

(21) Sanchez Fernandez, E.; Goetheer, E. L. V.; Manzolini, G.; Macchi, E.; Rezvani, S.; Vlugt, T. J. H. Thermodynamic assessment of amine based CO2 capture technologies in power plants based on European Benchmarking Task Force methodology,. *Fuel* **2014**, *129*, 318−329.

(22) Manzolini, G.; Sanchez Fernandez, E.; Rezvani, S.; Macchi, E.; Goetheer, E. L. V.; Vlugt, T. J. H. Economic assessment of novel amine based CO2 capture technologies integrated in power plants

based on European Benchmarking Task Force methodology,. *Appl. Energy* **2015**, *138*, 546−558.
(23) Abanades, J. C.; Arias, B.; Lyngfelt, A.; Mattisson, T.; Wiley, D. E.; Li, H.; Ho, M. T.; Mangano, E.; Brandani, S. Emerging CO2 capture systems,. *Int. J. Greenhouse Gas Control* **2015**, *40*, 126−166.
(24) Huang, J.; Zou, J.; Ho, W. S. W. Carbon Dioxide Capture Using a CO 2 -Selective Facilitated Transport Membrane,. *Ind. Eng. Chem. Res.* **2008**, *47*, 1261−1267.
(25) He, X.; Fu, C.; Hägg, M. B. Membrane system design and process feasibility analysis for CO2 capture from flue gas with a fixed-site-carrier membrane,. *Chem. Eng. J.* **2015**, *268*, 1−9.
(26) Sandru, M.; Kim, T.-J.; Capala, W.; Huijbers, M.; Hägg, M.-B. Pilot Scale Testing of Polymeric Membranes for CO2 Capture from Coal Fired Power Plants,. *Energy Procedia* **2013**, *37*, 6473−6480.
(27) Sipöcz, N.; Tobiesen, F. A. Natural gas combined cycle power plants with CO2 capture − Opportunities to reduce cost,. *Int. J. Greenhouse Gas Control* **2012**, *7*, 98−106.
(28) Lindqvist, K.; Jordal, K.; Haugen, G.; Hoff, K. A.; Anantharaman, R. Integration aspects of reactive absorption for post-combustion CO2 capture from NGCC (natural gas combined cycle) power plants,. *Energy* **2014**, *78*, 758−767.
(29) Li, H.; Ditaranto, M.; Berstad, D. Technologies for increasing CO2 concentration in exhaust gas from natural gas-fired power production with post-combustion, amine-based CO2 capture,. *Energy* **2011**, *36*, 1124−1133.
(30) Evulet, A. T.; El Kady, A. M.; Branda, A. R.; Chinn, D. On the Performance and Operability of GE's Dry Low NOx Combustors utilizing Exhaust Gas Recirculation for PostCombustion Carbon Capture,. *Energy Procedia* **2009**, *1*, 3809−3816.
(31) Van der Spek, M.; Ramirez, A.; Faaij, A. Challenges and uncertainty of ex ante techno-economic analysis of low TRL CO2 capture technology: Lessons from the case study of NGCC with Exhaust Gas Recycle and Electric Swing Adsorption,. *Appl. Energy* **2017**, *208*, 920−934.
(32) *Thermoflex*; Thermoflow: Southborough, MA, USA, 2016.
(33) Van Hassel, B. A. Oxygen transfer across composite oxygen transport membranes,. *Solid State Ionics* **2004**, *174*, 253−260.
(34) Merkel, T. C.; Lin, H.; Wei, X.; Baker, R. Power plant post-combustion carbon dioxide capture: An opportunity for membranes,. *J. Membr. Sci.* **2010**, *359*, 126−139.
(35) Kvamsdal, H. M.; Rochelle, G. T. Effects of the Temperature Bulge in CO 2 Absorption from Flue Gas by Aqueous Monoethanolamine,. *Ind. Eng. Chem. Res.* **2008**, *47*, 867−875.
(36) Merkel, T. C. *Personal communication*, 13th International Conference on Greenhouse Gas Control Technologies, Lausanne, Switzerland, Nov. 14−18, 2016.
(37) Ceccarelli, N.; et al. Flexibility of low-CO2 gas power plants: Integration of the CO2 capture unit with CCGT operation,. *Energy Procedia* **2014**, *63*, 1703−1726.
(38) Bui, M.; Gunawan, I.; Verheyen, V.; Feron, P.; Meuleman, E.; Adeloju, S. Dynamic modelling and optimisation of flexible operation in post-combustion CO2 capture plants—A review,. *Comput. Chem. Eng.* **2014**, *61*, 245−265.
(39) Roeder, V.; Hasenbein, C.; Kather, A. Evaluation and Comparison of the Part Load Behaviour of the CO2 Capture Technologies Oxyfuel and Post-Combustion,. *Energy Procedia* **2013**, *37*, 2420−2431.
(40) Rubin, E. S.; et al. A proposed methodology for CO2 capture and storage cost estimates,. *Int. J. Greenhouse Gas Control* **2013**, *17*, 488−503.
(41) DOE/NETL. *Quality Guidelines for Energy Systems Studies: Capital Cost Scaling Methodology*, Report DOE/NETL-341/013113; Department of Engergy/National Energy Technology Laboratory (DOE/NETL): Pittsburgh, PA, 2013.
(42) Van der Sluijs, J. P.; Hendriks, C. A.; Blok, K. Feasibility of polymer membranes for carbon dioxide recovery from flue gases,. *Energy Convers. Manage.* **1992**, *33*, 429−436.
(43) Knoope, M. M. J.; Guijt, W.; Ramírez, A.; Faaij, A. P. C. Improved cost models for optimizing CO2 pipeline configuration for point-to-point pipelines and simple networks,. *Int. J. Greenhouse Gas Control* **2014**, *22*, 25−46.
(44) Zhao, L.; Riensche, E.; Blum, L.; Stolten, D. Multi-stage gas separation membrane processes used in post-combustion capture: Energetic and economic analyses,. *J. Membr. Sci.* **2010**, *359*, 160−172.
(45) Lew, D.; et al. *The Western Wind and Solar Integration Study Phase 2*, Technical Report NREL/TP-5500-58798; National Renewable Energy Laboratory: Golden, CO, USA, 2013.
(46) Morken, A. K.; Pedersen, S.; Kleppe, E. R.; Wisthaler, A.; Vernstad, K.; Ullestad, Ø; Fløe, N. E.; Faramarzi, L.; Hamborg, E. S. Emission results of amine plant operations from MEA testing at the CO 2 Technology Centre Mongstad,. *Energy Procedia* **2017**, *114*, 1245−1262.
(47) Knudsen, J. N.; Andersen, J.; Jensen, J. N.; Biede, O. Evaluation of process upgrades and novel solvents for the post combustion CO2 capture process in pilot-scale,. *Energy Procedia* **2011**, *4*, 1558−1565.
(48) Mertens, J.; Knudsen, J.; Thielens, M.-L.; Andersen, J. On-line monitoring and controlling emissions in amine post combustion carbon capture: A field test,. *Int. J. Greenhouse Gas Control* **2012**, *6*, 2−11.
(49) Rieder, A.; Unterberger, S. EnBW's post-combustion capture pilot plant at heilbronn results of the first year's testing programme,. *Energy Procedia* **2013**, *37*, 6464−6472.
(50) Hussain, A.; Hägg, M.-B. A feasibility study of CO2 capture from flue gas by a facilitated transport membrane,. *J. Membr. Sci.* **2010**, *359*, 140−148.